Astronomy & Astrophysics manuscript no. draft˙140222
February 25, 2014
© ESO 2014

arXiv:1402.5526v1 [astro-ph.CO] 22 Feb 2014

Effects of the environment on galaxies in the Catalogue of Isolated Galaxies: physical satellites and large scale structure

M. Argudo-Fernández[1,2], S. Verley[2], G. Bergond[3], J. Sulentic[1], J. Sabater[4], M. Fernández Lorenzo[1], D. Espada[5,6,7], S. Leon[5], S. Sánchez-Expósito[1], J. D. Santander-Vela[1], and L. Verdes-Montenegro[1]

[1] Instituto de Astrofísica de Andalucía (CSIC) Apdo. 3004, 18080 Granada, Spain
[2] Departamento de Física Teórica y del Cosmos, Universidad de Granada, 18071 Granada, Spain
[3] Centro Astronómico Hispano Alemán, Calar Alto, (CSIC-MPG), C/ Jesús Durbán Remón 2-2, E-04004 Almería, Spain
[4] Institute for Astronomy, University of Edinburgh, Edinburgh EH9 3HJ, UK
[5] Joint ALMA Observatory (ALMA/ESO), Alonso de Córdova 3107, Vitacura, Santiago 763-0355, Chile
[6] National Astronomical Observatory of Japan (NAOJ), 2-21-1 Osawa, Mitaka, Tokyo 181-8588, Japan
[7] Department of Astronomical Science, The Graduate University for Advanced Studies (SOKENDAI), 2-21-1 Osawa, Mitaka, Tokyo 181-8588, Japan

Received August 16, 2013; accepted February 22, 2014

ABSTRACT

Context. We present a study of the 3-dimensional environment for a sample of 386 galaxies in the **C**atalogue of **I**solated **G**alaxies (CIG, Karachentseva 1973) using the Ninth Data Release of the Sloan Digital Sky Survey (SDSS-DR9).
Aims. We aim to identify and quantify the effects of the satellite distribution around a sample of galaxies in the CIG, as well as the effects of the Large Scale Structure (LSS).
Methods. To recover the physically bound galaxies we first focus on the satellites which are within the escape speed of each CIG galaxy. We also propose a more conservative method using the stacked Gaussian distribution of the velocity difference of the neighbours. The tidal strengths affecting the primary galaxy are estimated to quantify the effects of the local and LSS environments. We also define the projected number density parameter at the 5th nearest neighbour to characterise the LSS around the CIG galaxies.
Results. Out of the 386 CIG galaxies considered in this study, at least 340 (88% of the sample) have no physically linked satellite. Following the more conservative Gaussian distribution of physical satellites around the CIG galaxies leads to upper limits. Out of the 386 CIG galaxies, 327 (85% of the sample) have no physical companion within a projected distance of 0.3 Mpc. The CIG galaxies are distributed following the LSS of the local Universe, although presenting a large heterogeneity in their degree of connection with it. When present around a CIG galaxy, the effect of physically bound galaxies largely dominates (usually by more than 90%) the tidal strengths generated by the LSS.
Conclusions. The CIG samples a variety of environments, from galaxies with physical satellites to galaxies with no neighbours within 3 Mpc. A clear segregation appears between early-type CIG galaxies with companions and isolated late-type CIG galaxies. Isolated galaxies are in general bluer, with likely younger stellar populations and rather high star formation with respect to older, redder CIG galaxies with companions. Reciprocally, the satellites are redder and with an older stellar populations around massive early-type CIG galaxies, while they have a younger stellar content around massive late-type CIG galaxies. This suggests that the CIG is composed of a heterogeneous population of galaxies, sampling from old to more recent, dynamical systems of galaxies. CIG galaxies with companions might have a mild tendency (0.3-0.4 dex) to be more massive, and may indicate a higher frequency of having suffered a merger in the past.

Key words. galaxies: general – galaxies: fundamental parameters – galaxies: formation – galaxies: evolution – galaxies: environment – galaxies: isolation

1. Introduction

Isolated galaxies are located, by definition, in low-density regions of the Universe, and should not be significantly influenced by their neighbours. Does a separate population of isolated galaxies exist, or are isolated galaxies simply the least clustered galaxies of the Large Scale Structure (LSS)? It is assumed that over the past several billion years the evolution of these objects has largely been driven by internal processes. A significant population of isolated galaxies is of great interest for testing different scenarios of the origin and evolution of galaxies. In this sense, isolated galaxies are an ideal sample of reference for studying the effects of environment on different galaxy properties. Such a sample would represent the most nurture-free galaxy population.

Studies of isolated galaxies can be argued to begin with the publication of the Catalogue of Isolated Galaxies (CIG; Karachentseva 1973). The AMIGA (**A**nalysis of the interstellar **M**edium of **I**solated **GA**laxies[1]) project (Verdes-Montenegro et al. 2005) is based upon a re-evaluation of the CIG. It is a first step in trying to identify and better characterise isolated galaxies in the local Universe. Verdes-Montenegro et al. (2005) argued that 50% or more galaxies in the CIG show a homogeneous redshift distribution. Sulentic et al. (2006), and more recently Fernández Lorenzo et al. (2012), found that 2/3 of the CIG are Sb-Sc late-type galaxies, and 14% are early-type. This implies an extremely high late-type fraction and extremely low early-type population. At intermediate redshift, Cooper et al. (2012)

[1] `http://amiga.iaa.es`

found that early-type systems in higher density regions tend to be more extended than their counterparts in low density environments. Taking into account the effect of the local environment, Fernández Lorenzo et al. (2013) show that the number of satellites around a galaxy affects its size. CIG galaxies have larger sizes than galaxies in the Nair & Abraham (2010) sample with zero or one satellite, which are also larger than galaxies in Nair & Abraham (2010) with two or more satellites.

The distribution of satellites (faint companions) around isolated primary galaxies provides important information about galaxy formation, as well as a critical test of the ΛCDM model on small scales (Einasto & Einasto 1987; Choi et al. 2007; Agustsson & Brainerd 2010; Ferrero et al. 2012; Anderhalden et al. 2013; Bozek et al. 2013). This explains the growing interest for studying the satellite distribution (Prada et al. 2003; Sales & Lambas 2005; Guo et al. 2012), and for exploring the link between galaxy properties and the satellite population (Park et al. 2007; Guo et al. 2011; Karachentseva et al. 2011; Edman et al. 2012; González et al. 2013).

According to a previous study (Argudo-Fernández et al. 2013), the criteria proposed by Karachentseva (1973) to remove fore- and background galaxies are not fully efficient. About 50% of the neighbours, considered as potential companions, have very high recession velocities with respect to the central CIG galaxy: the condition is too restrictive, and may consider as not isolated galaxies slightly affected by their environment. On the other hand, about 92% of neighbour galaxies showing recession velocities similar to the corresponding CIG galaxy are not considered as potential companions by the CIG isolation criteria, and may have a non negligible influence on the evolution of the central CIG galaxy. This motivates us to extend the study, taking into account nearby and similar redshift companions to identify physical satellites affecting the evolution of the central CIG galaxy, so as to provide a more physical estimation of the isolation degree of the CIG. About 60% of the CIG galaxies have no major (similar-size) companion in the SDSS, according to the CIG (purely photometric) isolation criteria. Nevertheless, considering the third dimension, only 1/3 of the sample has no similar redshift neighbours (Argudo-Fernández et al. 2013).

In this context the CIG represents an excellent sample to study the relation of galaxy properties on both local and large-scale environments.

In the present work, we aim to identify and quantify the effects of the satellite distribution around a sample of CIG galaxies, as well as the effects of the Large Scale Structure. This study is organised as follows: in Sect. 2, the sample and the data used are presented. The method to identify the potential satellite galaxies is described in Sect. 3. In Sect. 4, we describe the parameters used to quantify the environment. We present our results in Sect. 5 and the associated discussion in Sect. 6. Finally a summary and the main conclusions of the study are presented in Sect. 7. Throughout the study, a cosmology with $\Omega_{\Lambda 0} = 0.7$, $\Omega_{\mathrm{m}0} = 0.3$, and $H_0 = 70\,\mathrm{km\,s^{-1}\,Mpc^{-1}}$ is assumed.

2. The sample and the data

The CIG (Karachentseva 1973) has been assembled with the requirement that no similar size galaxy i with angular diameter D_i between 1/4 and 4 times the apparent diameter D_P of the primary CIG galaxy lies within $20\,D_i$ (Eqs. 1 and 2):

$$\frac{1}{4}\,D_P \leq D_i \leq 4\,D_P \quad ; \tag{1}$$

$$R_{iP} \geq 20\,D_i \quad . \tag{2}$$

Until recently, most of the identifications and evaluations of large samples of isolated galaxies have been carried out using photometric data. The advent of the Sloan Digital Sky Survey (SDSS; York et al. 2000; Eisenstein et al. 2011) has opened up the possibility to develop a detailed spectroscopic study of the environment of galaxies in the CIG.

Our starting sample is based on the CIG galaxies found in the ninth data release (DR9; Ahn et al. 2012) of the SDSS. We focus our study on CIG galaxies with recession velocities $v \geq 1500\,\mathrm{km\,s^{-1}}$ (Verley et al. 2007b) so as to avoid an overwhelmed search for potential neighbours (the angular size on the sky for 1 Mpc at a distance of $1500\,\mathrm{km\,s^{-1}}$ is approximately 2.°9). We then add the requirement that more than 80% of the neighbours within a projected radius of 1 Mpc possess a spectroscopic redshift in either the main galaxy sample (Strauss et al. 2002), with magnitudes between $14.5 < m_{r,\mathrm{Petrosian}} < 17.77$, or in the Baryon Oscillation Spectroscopic Survey (BOSS; Dawson et al. 2013) which uses a new spectrograph (Smee et al. 2012) to obtain spectra of galaxies with $0.15 < z < 0.8$ and quasars with $2.15 < z < 3.5$, thus useful to reject background objects in our study. To correct for redshift incompleteness in the field, we use the photometric redshift z_p provided by the SDSS (z of the table Photoz, for galaxies at magnitudes $m_r < 17.77$ according to Sabater et al. 2013). After a first rejection of neighbours with $z_p > 0.1$ as background galaxies, we select as potential companions neighbour galaxies with $|z_{\mathrm{CIG}} - z_p| < 2.5\,z_{p,\mathrm{Err}}$ (Guo et al. 2011), where z_{CIG} is the spectroscopic redshift of the CIG galaxy and $z_{p,\mathrm{Err}}$ is the photometric redshift error.

In order to evaluate the effects of the large scale environment, we follow a methodology similar to Argudo-Fernández et al. (2013), searching for neighbours around 386 CIG fields completely covered by the SDSS within a physical projected radius of 3 Mpc.

Model magnitudes in the r-band (the deepest images) are used in our study. Sizes are estimated from r_{90}, the Petrosian radius containing 90 % of the total flux of the galaxy in the r-band[2], as explained in Argudo-Fernández et al. (2013). Absolute magnitudes and stellar masses (see upper panel in Fig. 1) for both CIG galaxies and neighbours, are calculated by fitting the spectral energy distribution using the routine kcorrect (Blanton & Roweis 2007).

3. Identification of physical companions

To recover the physical satellites around the CIG galaxies, we first focus on the satellites which are within the escape speed of each CIG galaxy (Sect. 3.1). We also propose a more conservative method using the stacked Gaussian distribution of the velocity difference of the neighbours, with respect to the corresponding CIG galaxy, which gives an upper limit for the influence of the local environment (Sect. 3.2).

3.1. Escape speed

To identify the physical satellites which may have had a secular influence on the central CIG galaxy, we use the escape speed in order to select the physically bound satellite galaxies. The escape speed at a given distance reads:

$$v_{\mathrm{esc}} = \sqrt{\frac{2GM_P}{R_{iP}}} \quad , \tag{3}$$

[2] http://www.sdss3.org/dr9/algorithms/magnitudes.php

where G is the universal gravitational constant, M_P is the dynamical mass of the central CIG galaxy, and R_{iP} is the distance between the neighbour i and the primary galaxy P.

In the upper panel of Fig. 1, the distribution of the stellar masses of the CIG galaxies is presented. The logarithm of the stellar mass spans 8.1–11.4 $M_\odot$, with a peak towards 10.5 $M_\odot$. The dynamical masses of the CIG galaxies are estimated from their stellar masses following the parametrisation in Moster et al. (2013), including redshift evolution (see their Eq. 2). The result of the Stellar-to-Halo Mass (SHM) parametrisation for CIG galaxies is shown in middle and lower panels in Fig. 1.

The escape separation should be computed using the 3-dimensional space between the central CIG galaxy and its neighbours. Unfortunately we do not have this information and the use of projected separations, as well as 1-dimensional line-of-sight velocities, would lead to an overestimation of the number of physical companions. To correct for this bias we first assume an isotropic velocity distribution (see also next section). Under this hypothesis, the 1-dimensional, line-of-sight velocity is related to the 3-dimensional velocity by a scale factor $\sqrt{3}$. Similarly, the projected separation should be multiplied by a factor $\frac{\sqrt{3}}{\sqrt{2}}$ to approximate 3D separation. Although these approximations may not be totally exact for a given CIG galaxy, they nevertheless represent a useful first step towards a full 3D characterisation of the environment of galaxies.

Several levels of the escape speed are shown in the upper panel of Fig. 2, as a function of the projected distance, up to 0.3 Mpc. The levels are calculated for a typical stellar mass of $10^{10.5}$ $M_\odot$, translating into a dynamical mass of $10^{11.9}$ $M_\odot$. In the lower panel, we show the characteristic trumpet shape (caustic Kaiser 1987; Strauss & Willick 1995; Diaferio & Geller 1997) under which the satellite galaxies would be captured. Above the caustic, the neighbour galaxies possess a velocity sufficient to evade the gravitational attraction of the primary galaxy and are not captured, although fly-by interactions may influence the structure and evolution of the primary galaxy.

Using the escape speed, the satellite galaxies considered physically bound with their corresponding CIG galaxy, are all neighbours satisfying the condition $|\Delta v| \leq \sqrt{\frac{2GM_P}{3\frac{\sqrt{3}}{\sqrt{2}}R_{iP}}}$ km s^{-1} and lying at a distance lower than 0.3 Mpc.

3.2. Gaussian distribution of physical satellites

Some galaxies may pass nearby a primary CIG galaxy, but with a velocity so high that they interact once with the CIG galaxy and then leave. To take into account the potential effect of fly-by encounters, we develop a more conservative method to recover most of the galaxies which have interacted with the CIG galaxies. We do so by stacking all the primaries and their satellites in order to obtain statistically robust results.

In the upper panel of Fig. 3, we show the distribution of the absolute values of the radial velocity difference between the projected neighbour galaxies and the central CIG galaxies ($\Delta v = v_{\rm neigh} - v_{\rm CIG}$). Two components appear clearly in the figure. The first component is a flat continuum distribution of foreground/background neighbours, extending to Mpc scales, and related to the LSS distribution of galaxies. The second component is the over-abundance of neighbour galaxies peaking at $|\Delta v| = 0$ km s^{-1}; most of those would be dynamically related to the central CIG galaxies. In order to estimate the standard deviation, σ, of the distribution, we first estimate the median level of the background between 300 and 1000 km s^{-1}, and remove it. A

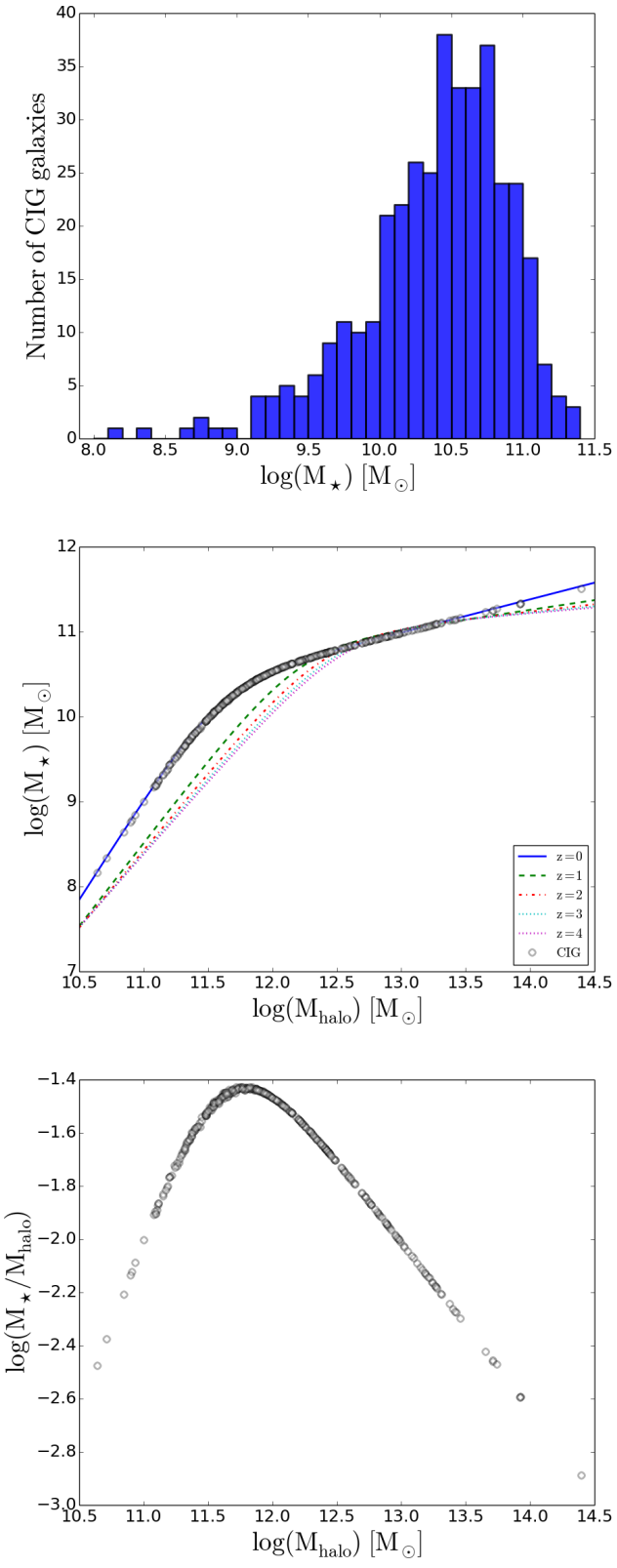

Fig. 1. *(upper panel):* Distribution of the stellar masses of the CIG galaxies. *(middle panel):* SHM relation for central galaxies as a function of redshift (Figure 5 in Moster et al. 2013). Blue solid line, green dashed line, red point-dashed line, cyan pointed line, and magenta pointed line correspond to the SHM relation at redshift 0, 1, 2, 3, and 4, respectively. Black circles correspond to the parametrisation of the SHM relation for CIG galaxies. *(lower panel):* Logarithm of the SHM ratio for CIG galaxies.

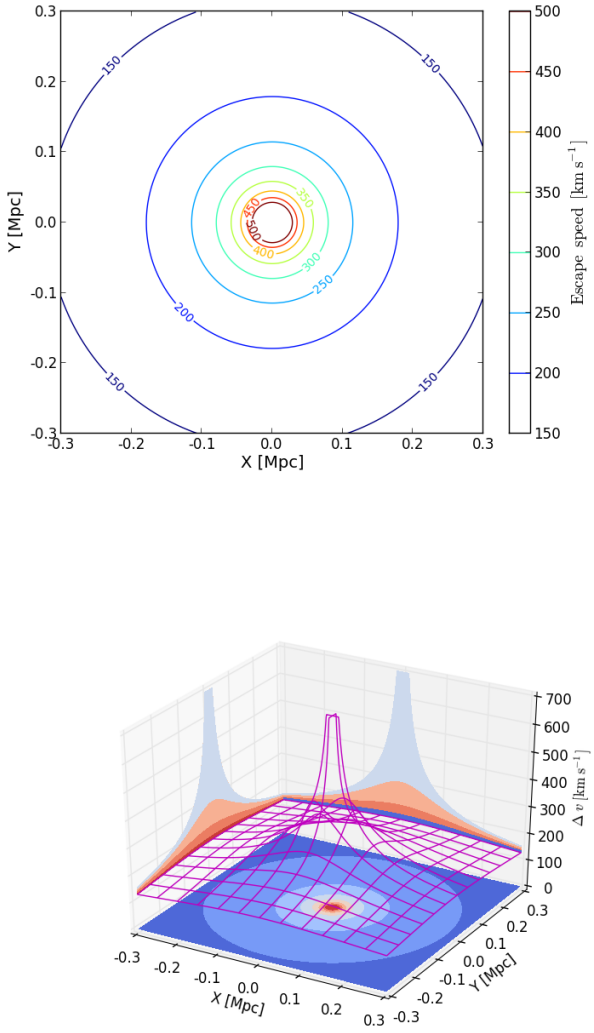

Fig. 2. *(upper panel):* 2-Dimensional escape speed schema in celestial coordinates space. The physically linked associations correspond to neighbour galaxies at distance to the central CIG galaxy and $|\Delta v|$ less than the corresponding value according to circle lines. The levels are calculated for a typical stellar mass of $10^{10.5}$ M$_\odot$, translating into a dynamical mass of $10^{11.9}$ M$_\odot$. *(lower panel):* 3-Dimensional escape velocity schema in a redshift-space diagram (line-of-sight velocity versus projected distance). The physically linked associations correspond to neighbour galaxies under the 'trumpet' surface. The levels are calculated for a typical stellar mass of $10^{10.5}$ M$_\odot$, translating into a dynamical mass of $10^{11.9}$ M$_\odot$.

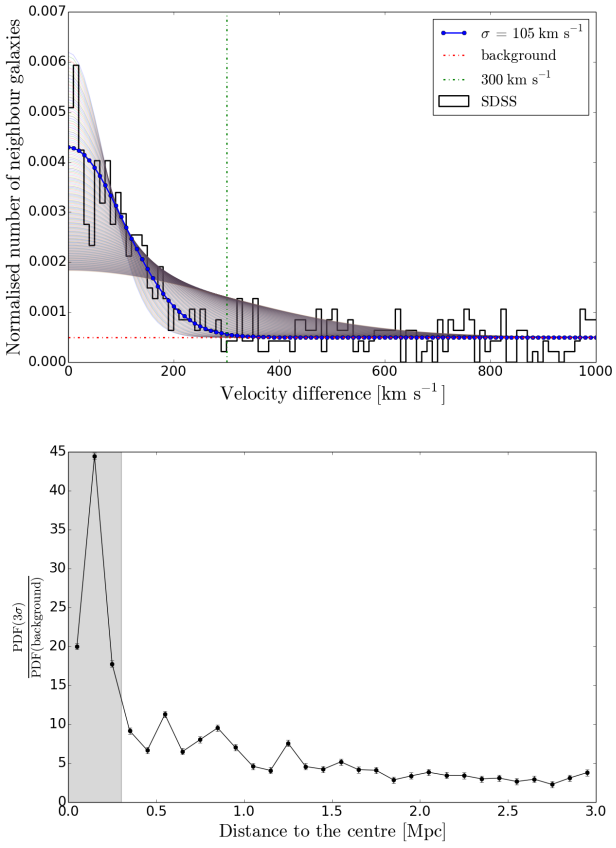

Fig. 3. *(upper panel):* Absolute values of the line-of-sight velocity difference between neighbours and the central CIG galaxy: $|\Delta v|$ distribution obtained by stacking 411 CIG fields within 1 Mpc field radius (black histogram), and corresponding Gaussian distribution fits for σ between 70 and 300 km s^{-1} (grey curves) with the best fit (blue curve). The Gaussian fit has been done within $|\Delta v| = 300$ km s^{-1} (vertical line) and considering as a zero point the flat continuum distribution of background neighbours (horizontal line). *(lower panel):* Probability Density Function (PDF) for neighbour galaxies peaking at $|\Delta v| = 0$ km s^{-1} over PDF for the background flat population selected in the interval $1000 < |\Delta v| < 3000$ km s^{-1}, as a function of the distance to the central CIG galaxy. The inner 0.3 Mpc are shaded.

Gaussian distribution appears for velocity differences minor than 300 km s^{-1}. We vary σ between 70 and 300 km s^{-1} and use a χ^2 fitting minimisation to obtain the standard deviation of the satellite distribution: $\sigma = 105$ km s^{-1}. Consequently, the 3σ limit is at 315 km s^{-1}. The neighbour galaxies with $|\Delta v| \leq 315$ km s^{-1} show a substantial liability to gather in the inner 0.3 Mpc around the CIG galaxies (see the lower panel of Fig. 3). This dynamical link is also confirmed by the constancy of the standard deviation for radii lower than 0.3 Mpc (see the upper panel of Fig. 6, and the associated analysis in Sect. 5.4). To be very conservative and recover 99.7% of the physically linked companions, we consider that all neighbours within $|\Delta v| \leq 3\sigma$ may be physically bound with their corresponding CIG galaxy.

Hence, the satellite galaxies selected by the Gaussian distribution are all neighbour galaxies with $|\Delta v| \leq 315$ km s^{-1} and lying at a distance lower than 0.3 Mpc. This method provides an upper limit on the quantification of the local environment, since more galaxies will be considered as satellites with respect to those selected following the escape speed method.

4. Quantification of the environment

In order to quantify the isolation degree of the CIG galaxies, we use two complementary parameters: the tidal strength Q that the neighbours produce on the central galaxy (Verley et al. 2007a;

Sabater et al. 2013; Argudo-Fernández et al. 2013), and the projected density η_k (Eqs. 5 and 6) of neighbour galaxies considered in this study.

4.1. Tidal strength parameter

The tidal strength parameter is defined as:

$$Q_{iP} \equiv \frac{F_{\rm tidal}}{F_{\rm bind}} \propto \frac{M_i}{M_P}\left(\frac{D_P}{R_{iP}}\right)^3 \quad , \tag{4}$$

where M_i and M_P are the stellar masses of the neighbour and the principal galaxy, respectively, D_P the apparent diameter of the principal galaxy, and R_{iP} the projected physical distance between the neighbour and principal galaxy. We use the apparent diameter $D_P = 2\,r_{90}$ scaled by a factor 1.43 (Argudo-Fernández et al. 2013) to match the definition of diameter used in the literature (projected major axis of a galaxy at the 25 mag arcsec^{-2} isophotal level or D_{25}, Verley et al. 2007a). The total tidal strength is then defined as:

$$Q = \log\left(\sum_i Q_{iP}\right) \quad . \tag{5}$$

The logarithm of the sum of the tidal strength created by all the neighbours in the field is a dimensionless estimation of the gravitational interaction strength (Verley et al. 2007a). The greater the value of Q, the less isolated from external influence the galaxy, and vice-versa.

4.2. Projected number density parameter

To characterise the LSS around the CIG galaxies, we also define the projected number density parameter (Verley et al. 2007a; Argudo-Fernández et al. 2013), as follows:

$$\eta_{k,\rm LSS} \propto \log\left(\frac{k-1}{V(r_k)}\right) \quad , \tag{6}$$

where $V(r_k) = \frac{4}{3}\,\pi\,r_k^3$ and r_k is the projected physical distance to the $k^{\rm th}$ nearest neighbour, with k equal to 5, or less if there were not enough neighbours in the field. The farther the $k^{\rm th}$ nearest neighbour, the smaller the projected number density $\eta_{k,\rm LSS}$.

5. Results

5.1. Spectroscopic identification of physical satellites around galaxies in the CIG

Out of the 386 CIG galaxies considered in this study, 340 have no physically linked satellites, which represents 88% of the sample. Among the 46 CIG galaxies with at least one physical companion within its escape speed boundary, 36 have one satellite, nine have two satellites, and one has three satellites (CIG 771). There is no CIG galaxy with more than three physically linked satellites. The values of the tidal forces exerted by these satellites on the CIG galaxies are listed in columns 2, 3, 4, and 5 of Table 1.

Following the more conservative Gaussian distribution of physical satellites around the CIG galaxies leads to upper limits. Out of the 386 CIG galaxies, 327 (85% of the sample) have no physical companion within a projected distance of 0.3 Mpc. Out of the remaining 59 CIG galaxies (15%), 46, 11, and 2 CIG galaxies (CIG 237 and CIG 771) are in interaction with one, two, and three physical companions, respectively.

Examples of the environment for three CIG galaxies are shown in Fig. 4. CIG 203 has no physically bound companions. On the other hand, CIG 401 and CIG 771 are linked locally with companions that are caught under their gravitational influence.

5.2. Correction for the redshift incompleteness

As mentioned in Sect. 2, the sample used in this study was selected for CIG fields with at least 80% redshift completeness (the mean completeness of the sample is 92.5%). Therefore, to correct for this incompleteness we consider photometric redshifts to compensate the estimation of the local environment. The upper limit on the local tidal strength is then calculated considering the potential companions at the same distance as their corresponding CIG galaxy, i.e., the least favourable case for the isolation degree.

This correction is applied to the already conservative Gaussian distribution selection of physical satellites, introducing no change for 356 CIG galaxies (92% of the sample). Out of the remaining 30 CIG galaxies, 22 CIG galaxies without satellite acquire one, six CIG galaxies pass from one to two satellites, and one CIG galaxy passes from two to three satellites. Only one CIG galaxy, CIG 626, gains more than one possible satellite, passing from none to three possible satellites.

The inclusion of one missing redshift galaxy as a potential companion increases the tidal strength by a mean value of 13%, with respect to the tidal strength generated by the spectroscopic satellites. The most unfavourable cases occur for CIG 278 and CIG 495 where the effect of the missing galaxy amounts to 64% and 83%, respectively.

5.3. Large Scale Structure

To quantify the large scale environment around the CIG galaxies, we use the two isolation parameters defined in Sect. 4. The parameter $Q_{\rm LSS}$ was calculated taking into account all companions within 3 Mpc and $|\Delta\,v| < 315\,{\rm km\,s^{-1}}$ to provide the sum of the tidal strengths exerted on the CIG galaxies. The parameter $\eta_{k,\rm LSS}$ accounts for the number density of companions within $|\Delta\,v| < 315\,{\rm km\,s^{-1}}$ and projected at the distance of the 5$^{\rm th}$ nearest neighbour with respect to the CIG galaxy. Only 10 CIG galaxies (less than 3% of the sample) are farther away than 3 Mpc from any other galaxy with a SDSS measured spectrum.

In Fig. 5, the projected number density is shown versus the tidal strength parameter. Due to the logarithmic definition of the parameters, the figures appear to span several orders in magnitude (3 dex for $\eta_{k,\rm LSS}$ and 7 dex for $Q_{\rm LSS}$) showing the large scatter in the environments found around the CIG galaxies. The results of the quantifications of the environment are listed in columns 6, 7, and 8 of Table 1. CIG galaxies with physically bound satellites tend to show greater values of $Q_{\rm LSS}$ but not $\eta_{k,\rm LSS}$.

The large scale environment is graphically exemplified around three CIG galaxies in the right column of Fig. 4. There is a sparse population of galaxies in the LSS around CIG 203, while CIG 401 and CIG 771 show a much more crowded LSS within 3 Mpc.

5.4. Local environment versus large scale environment

To evaluate the role of the physically bound satellites with respect to the large scale environment, we compare the magnitudes of the sum of the tidal forces produced by the physical compan-

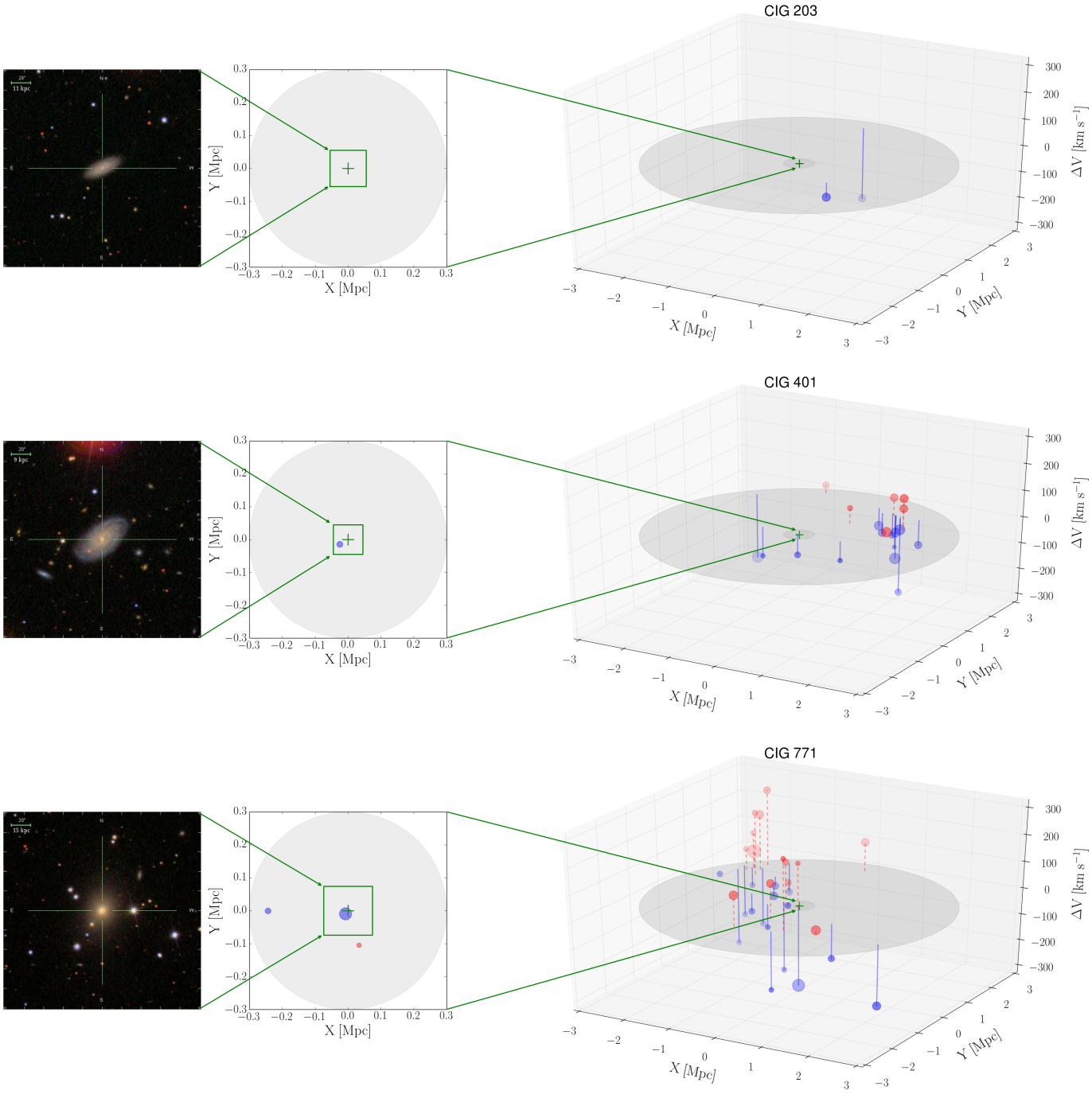

Fig. 4. SDSS three-colour images (left, with a field of view of 3′3, North is up, East is to the left), representation in 2D (center, with a field of view of 0.6 Mpc, North is up, East is to the left), and representation in 3D (right, with a field of view of 6 Mpc) of the environment of the galaxies CIG 203 (upper panel), CIG 401 (middle panel), and CIG 771 (lower panel). The central green pluses correspond to the locations of the primary CIG galaxies. Grey disks at 0.3 and 3 Mpc boundaries represent the areas to study the local environment and the LSS, respectively. The sizes of the symbols are proportional to the diameters of the neighbours (not at scale), in red or blue according to blueshift or redshift of the neighbours. Vertical lines indicate the projection of the neighbours in the 2-Dimensional plane. Solid green lines indicate the scale relations between the three different representations.

ions to the sum of the tidal forces engendered by all the galaxies in the LSS. When at least one physical companion is present near a CIG galaxy, its effect largely dominates (usually more than 90%) over the tidal forces generated by the LSS. This effect is clearly visible in Fig. 5. The ratios $Q_{\rm sat}/Q_{\rm LSS}$ and $Q_{\rm sat,sup}/Q_{\rm LSS}$ are tabulated in columns 9 and 10 of Table 1, respectively.

It seems that there is a natural distinction between the physically bound satellites and the LSS. This dichotomy appears for instance if we plot the standard deviation of a Gaussian fitting as a function of the projected distance (see the upper panel of Fig. 6). Up to ∼ 0.3 Mpc, most of the galaxies are linked to their host. If the systems have been in interaction long enough, they

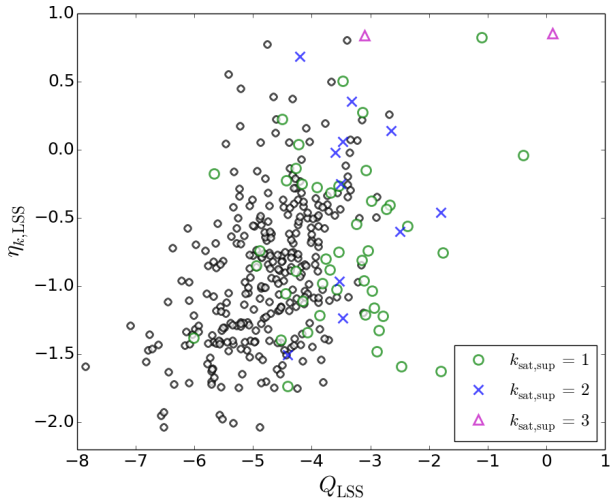

Fig. 5. Projected number density $\eta_{k,\mathrm{LSS}}$ versus tidal strength Q_{LSS} diagram for the LSS. CIG galaxies with one, two, and three dynamically linked satellites are depicted by green circles, blue crosses, and magenta triangles, respectively.

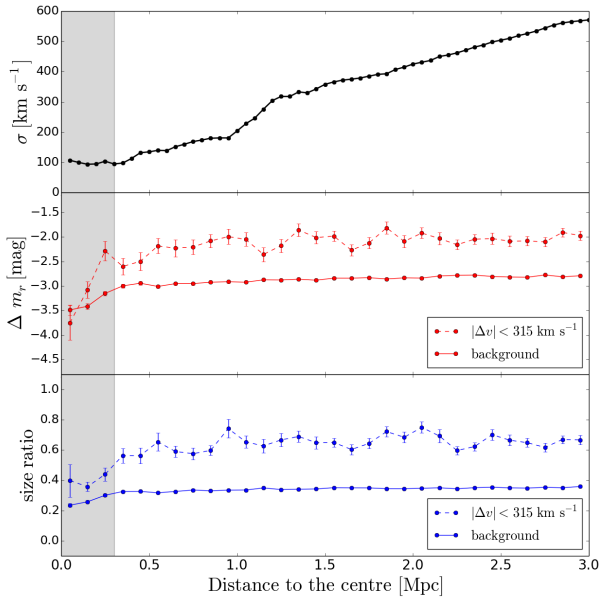

Fig. 6. *(upper panel):* Standard deviation σ of the Gaussian distribution fitting for $|\Delta\, v|$ as a function of the distance to the central galaxy. *(middle panel):* Magnitude difference ($\Delta\, m_r = m_r^P - m_r^i$ between neighbour i and its corresponding primary CIG galaxy P) for satellites ($|\Delta\, v| \leq 315\,\mathrm{km\,s^{-1}}$, red dashed line) and for background galaxies ($315 < |\Delta\, v| < 3000\,\mathrm{km\,s^{-1}}$, red solid line) as a function of the distance to the central CIG galaxy. *(lower panel):* Size ratio ($\frac{D_i}{D_P}$ between neighbour i and its corresponding primary CIG galaxy P) for satellites ($|\Delta\, v| \leq 315\,\mathrm{km\,s^{-1}}$, blue dashed line) and for the background population ($315 < |\Delta\, v| < 3000\,\mathrm{km\,s^{-1}}$, blue solid line) as a function of the distance to the central CIG galaxy. The inner 0.3 Mpc are shaded in the three panels.

are relaxed and the velocity differences are virialised. This appears as a plateau in the inner $\sim$ 0.3 Mpc, with a constant standard deviation $\sigma \approx 105\,\mathrm{km\,s^{-1}}$. At larger distances, the standard deviation monotonically increases due to the rising fraction of the LSS galaxies enclosed.

The physically captured satellite galaxies are typically 1.5 dex fainter than the magnitude of galaxies lying farther away (see the middle panel of Fig. 6). In average, the galaxies in the inner $\sim$ 0.3 Mpc are also smaller (about $0.4 \times D_P$) compared to galaxies which are not satellites ($\sim 0.7 \times D_P$).

The connection between the CIG and the LSS is revealed by comparing the apparent magnitudes and sizes of the galaxies with $|\Delta\, v| < 315\,\mathrm{km\,s^{-1}}$ to the ones of the galaxies outside this limit (see middle and lower panels of Fig. 6, respectively). Galaxies with similar velocities have magnitudes and sizes closer to the ones of CIG galaxies, compared to background and foreground galaxies (defined by galaxies with recession velocities in the range $315 < |\Delta\, v| < 3000\,\mathrm{km\,s^{-1}}$), disclosing the association between the CIG galaxies and their surrounding LSS.

6. Discussion

6.1. The construction of the CIG

In a previous work (Argudo-Fernández et al. 2013) we revised the CIG isolation criterion using both photometry and spectroscopy from the SDSS-DR9. We found that the 16% of the CIG galaxies considered in the spectroscopic study do not pass the CIG isolation criterion. There may be a population of very close physical satellites which may have a considerable influence on the evolution of the central CIG galaxy. Therefore, one of the aims of the present study is to characterise such a population of satellites.

As shown in Sect. 5.1, about 12% (and up to 15%) of the CIG galaxies have physically bound satellites. To seek why these systems are included in the CIG, it is worth to recall that the CIG has been constructed visually, on photographic material (Karachentseva 1973). Unfortunately, the sample of neighbour galaxies inspected originally is not available. Nevertheless, a revision has been carried out by Verley et al. (2007b) on the same original material (Palomar Observatory Sky Survey, POSS), providing a catalogue of approximately 54,000 neighbours. By comparing the physically bound satellites found in the SDSS to this POSS-based catalogue, we should be able to point out some drawbacks due to the use of photographic plates and the nearly total lack of redshift availability, forty years ago.

In the left panel of Fig. 7, we show that the SDSS identification of satellites goes, in general, deeper than the POSS. Indeed, Verley et al. (2007b) recover neighbour galaxies brighter than $B = 17.5$. The slight overlap of magnitudes between the two distributions is due to the non-linearity of the photographic material, as well as the varying zero-point from field to field in the POSS calibration (Verley et al. 2007b). Equally, in the central panel of Fig. 7, we see that the POSS search for companions misses the faintest galaxies, with respect to the magnitudes of the primary CIG galaxies.

Nonetheless, Karachentseva (1973) did not use any magnitude criterion to search for companions, and used only the apparent diameters of galaxies instead. In the right panel of Fig. 7, it is shown that about half of the physical companions missed by the POSS have diameters smaller than one fourth of the diameter

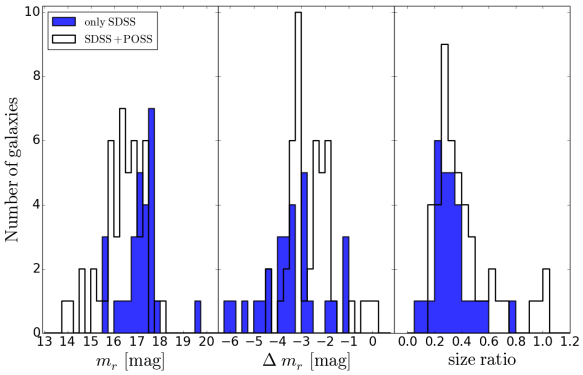

Fig. 7. Distribution of apparent magnitude (left panel), apparent magnitude difference (central panel), and size ratio (right panel) for physical linked satellites. Distributions for satellites which were not identified in the POSS (Verley et al. 2007b) are represented by blue histograms.

of their corresponding CIG galaxy, and were therefore not considered by the CIG isolation criteria. In fact, 23% of the missing physical companions are dwarf galaxies discarded by the original study. For instance, in the case of CIG 771, none of its three physically linked galaxies would violate the CIG isolation criterion. Nevertheless, its closest satellite, at 12 kpc and with a velocity difference of 230 km s^{-1}, tackled by the present study may have a considerable influence on the evolution of CIG 771. Redshift surveys are mandatory in order to distinguish small, faint, physically bound satellites from a background projected galaxy population.

6.2. Identification of satellites

Due to the spectroscopic redshift limit of the SDSS, analysing the satellite population around isolated galaxies is a challenge. We have some limitations to take into account. We are only able to detect bright neighbours (M 31 or M 33 like galaxies) and the brightest dwarfs (Large Magellanic Cloud and Small Magellanic Cloud like satellites) around most central galaxies. Nevertheless, the spectroscopic catalogue of the SDSS is complete to $m_r < 17.77$ mag, so we are always able to detect neighbours within $\Delta\, m_r \leq 2$ mag, even for the faintest CIG galaxy.

The spatial location of satellites with respect to their primary galaxies is uncertain due to redshift space distortions and projection effects. We follow a very conservative approach and use the projected separation between the neighbour and the CIG galaxy, providing a lower limit on the 3D distance between the two galaxies, which increases the number of potentially linked satellites taken into account by the escape speed and Gaussian distribution selections. This will translate on conservative higher limits for the isolation parameters.

In addition, the redshifts only account for the radial (line of sight) component of the peculiar velocities of the galaxies. Consequently, the velocity difference Δv supplies also a lower limit and exaggerates the number of physically related companions, in particular for the escape speed selection method. Nevertheless, the escape velocity method selects satellites minimising the effect of background objects, although there is an uncertainty about the total dynamical mass of the primary galaxy.

On the other hand, the Gaussian distribution method selects as satellites all neighbours within $|\Delta v| \leq 3\sigma$ and at projected physical distances to the central galaxy $d \leq 0.3$ Mpc. The 3σ cut ensures that we recover more than 99.7% of the physically associated satellites. This method includes also a fraction of fly-by encounters that may have an influence on the evolution of the primary galaxies. However, this is a compromise because, at the same time, it incorporates galaxies which are more likely located at 4.5 Mpc from the primary galaxy rather than at the same distance and with a velocity difference $\Delta v = 315$ km s^{-1} (following the lineal approximation of the Hubble law $v = H_0 D$). This explains why the Gaussian distribution provides an upper limit to the escape speed selection.

6.3. Local and large scale environments around CIG galaxies

Although only up to 15% of the CIG galaxies in the sample have physically bound satellite, almost all galaxies (97%) can be directly related to a LSS. The very large scatter in the quantification of the LSS (see the values spanned by $\eta_{k,\mathrm{LSS}}$ and Q_{LSS} in Fig. 5) shows that the CIG includes both galaxies dominated by their immediate environment as well as galaxies almost free from any external influence. In particular ten CIG galaxies are not associated to a LSS, at least within 3 Mpc: CIG 229, 245, 284, 318, 331, 541, 542, 546, 674, and 702 (see their three-colour images in Fig. 8).

The continuous distributions of the $\eta_{k,\mathrm{LSS}}$ and Q_{LSS} isolation parameters show that the CIG spans all the variety of environments between these two extreme cases. The connection of the CIG galaxies with the LSS is obvious due to the excess of similar redshift galaxies between 0.3 and 3 Mpc, as can be seen in the lower panel of Fig. 3. According to the middle and lower panels of Fig. 6, the large scale association is also noticeable due to higher number of brighter and bigger galaxies at redshift similar to those of the CIG galaxies, with respect to fainter, smaller background objects. Hence, the CIG galaxies are distributed following the LSS of the local Universe, although presenting a large heterogeneity in their degree of connection with it.

Some illustrations of the different environments around the CIG galaxies are shown in Fig. 4. Due to the large and roughly equivalent number of blue- and redshifted neighbour galaxies within the projected 3 Mpc, the galaxy CIG 771 may reside in the outskirts of a poor cluster. The galaxy CIG 401 seems to be located towards the edge of a LSS, such as a filament or a wall. On the other hand, the galaxy CIG 203 appears only mildly in relation with a LSS since only two LSS neighbours can be found in its environment. Its isolation parameters are very low ($\eta_{k,\mathrm{LSS}} = -1.94$ and $Q_{\mathrm{LSS}} = -5.65$) and its spatial location could be towards a void part of the local Universe. This environment is closer to the one of the ten galaxies for which we find no relation with the LSS within the first 3 Mpc. It is interesting to note that, out of the ten most isolated galaxies studied here, nine are clearly late type spirals showing symmetric morphologies, with no visible signs of interaction (see Fig. 8). Some of these galaxies could represent the closest remains of a fossil spiral population.

6.4. Influence of the environment on the evolution of the primary galaxies

To delimit the role of the environment on the physical properties of the galaxies we compare, within the CIG, the most isolated galaxies to the galaxies with companions. For this com-

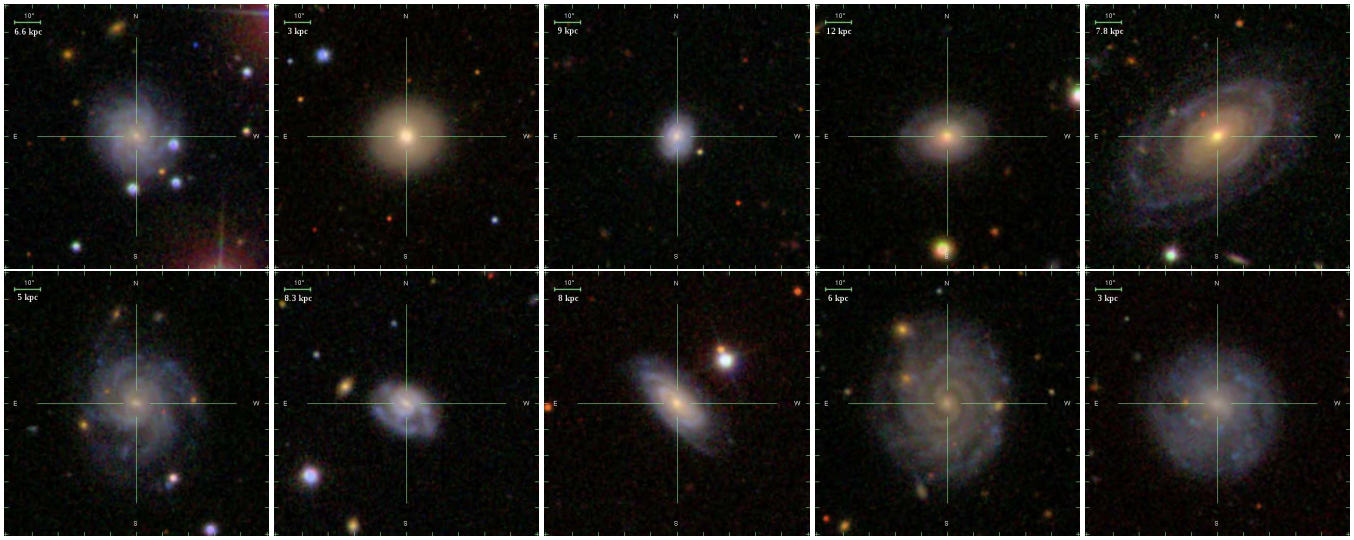

Fig. 8. SDSS three-colour images (field of view of 1.′7, North is up, East is to the left) of the ten most isolated CIG galaxies in the SDSS-DR9 footprint. From upper left to lower right: CIG 229, 245, 284, 318, 331, 541, 542, 546, 674, and 702.

parison, we use median values since they are less sensitive to outliers. Uncertainties are given by the 95% confidence interval of the median. The subsample of galaxies with companions encloses galaxies with at least one physically bound satellite in their vicinity ($k_{\rm sat}$ or $k_{\rm sat,sup}$ strictly positive). The subsample containing the most isolated CIG galaxies incorporates the galaxies presenting the lowest values of the projected number density ($\eta_{k,\rm LSS} < -1.5$) and tidal strength ($Q_{\rm LSS} < -6$), along with the ten galaxies isolated from both their local and LSS environments (CIG 229, 245, 284, 318, 331, 541, 542, 546, 674, and 702).

In the upper left panel of Fig. 9, the distribution of the logarithm of the stellar masses of the galaxies with companions (with median 10.70 ± 0.10) and isolated galaxies (with median 10.35 ± 0.17) are shown. Both subsamples extend from 10^9 to $10^{11.5}$ $M_\odot$, although the galaxies with companions might have a mild tendency (1σ) to be more massive, which may indicate a higher frequency of having suffered a merger in the past. Regarding the absolute magnitudes, the median for galaxies with companions is −21.48 ± 0.22 , while for isolated galaxies these values are −20.98 ± 0.27. There is no significant difference in the distributions of the absolute magnitudes between the two subsamples (upper central panel of Fig. 9).

Rest-frame colours $(g-r)$ and $(u-r)$ are derived from the absolute magnitudes in u-, g- and r-band, where $u = M_u$, $g = M_g$, and $r = M_r$ magnitudes are corrected for Galactic extinction (following the extinction maps from Schlegel et al. 1998) and k-correction. The median $(g - r)$ value for the galaxies with physically bound satellites is 0.76 ± 0.02, while the median value for the galaxies least affected by external tidal forces drops to 0.62 ± 0.05 (upper right panel of Fig. 9). This suggests that CIG galaxies with companions are in general redder and with older stellar populations with respect to the most isolated galaxies in the CIG which are bluer due to younger stellar populations (at a $\sim 2\sigma$ confidence level).

In the lower left panel of Fig. 9, the morphological T-types (Fernández Lorenzo et al. 2012) of the galaxies with companions and most isolated galaxies are shown. The fraction of early-type galaxies ($T < 0$) is dominated by galaxies with companions. On the other hand, the most isolated galaxies concentrate around the Sc type ($T = 5$), meaning that they are mainly late-type spiral galaxies. This trend is confirmed by the 10 most isolated galaxies: only one is early-type, while the remaining nine are consistently distributed around the Sc type. The inverse concentration index (ICI) defined as the ratio of the radii containing 50% and 90% of the Petrosian fluxes in the SDSS r-band, $C \equiv r_{p,50}/r_{p,90}$, is also an indicator of the morphological type. Early-type galaxies with a de Vaucouleurs profile will display values of the ICI around 0.3 while morphologies dominated by an exponential disk will show typical ICI values towards 0.43 (Strateva et al. 2001). The ICI histograms in the lower central panel of Fig. 9 confirm the trends based on the visual (optical) morphology: a marginal (1σ) segregation between early-type galaxies with companions (median 0.36 ± 0.02) and isolated late-type galaxies (median 0.42 ± 0.03). The intrinsic dispersion due to the use of the ICI as an estimation of the morphological type may also mix the two populations, which may be genuinely more separated. These tendencies can be related to the well known morphology-density relation for field and cluster galaxies (Dressler 1980; Dressler et al. 1997), but it is noteworthy to appreciate it even when the local environment is defined by only one, two, or three faint satellites.

The stellar populations of primary galaxies can be characterised in terms of $(u - r)$ rest-frame colours. In the lower right panel of Fig. 9, the well known SDSS-discovered bimodality appears, with an optimal separation at $(u - r) = 2.22$ (Strateva et al. 2001). Isolated galaxies mainly distribute in the range $(u - r) < 2.22$ (median 1.95 ± 0.16), while galaxies with companions spread over the area defined by $(u - r) > 2.22$ (median 2.48 ± 0.11). This segregation (with more than a 68% level of confidence) means that isolated galaxies are in general bluer, with a younger stellar population and rather high star formation with respect to older, redder galaxies with companions. These colours, in combination with morphological trends previously noticed and the $(g - r)$ colours, lead to a coherent view where isolated star forming galaxies are separated from older early-type galaxies with companions.

In Fig. 10, we show some mean properties of the physically linked satellites as a function of the stellar masses of the primary CIG galaxies, for two subsamples: physical satellites around early- and late-type CIG galaxies. The distribution of

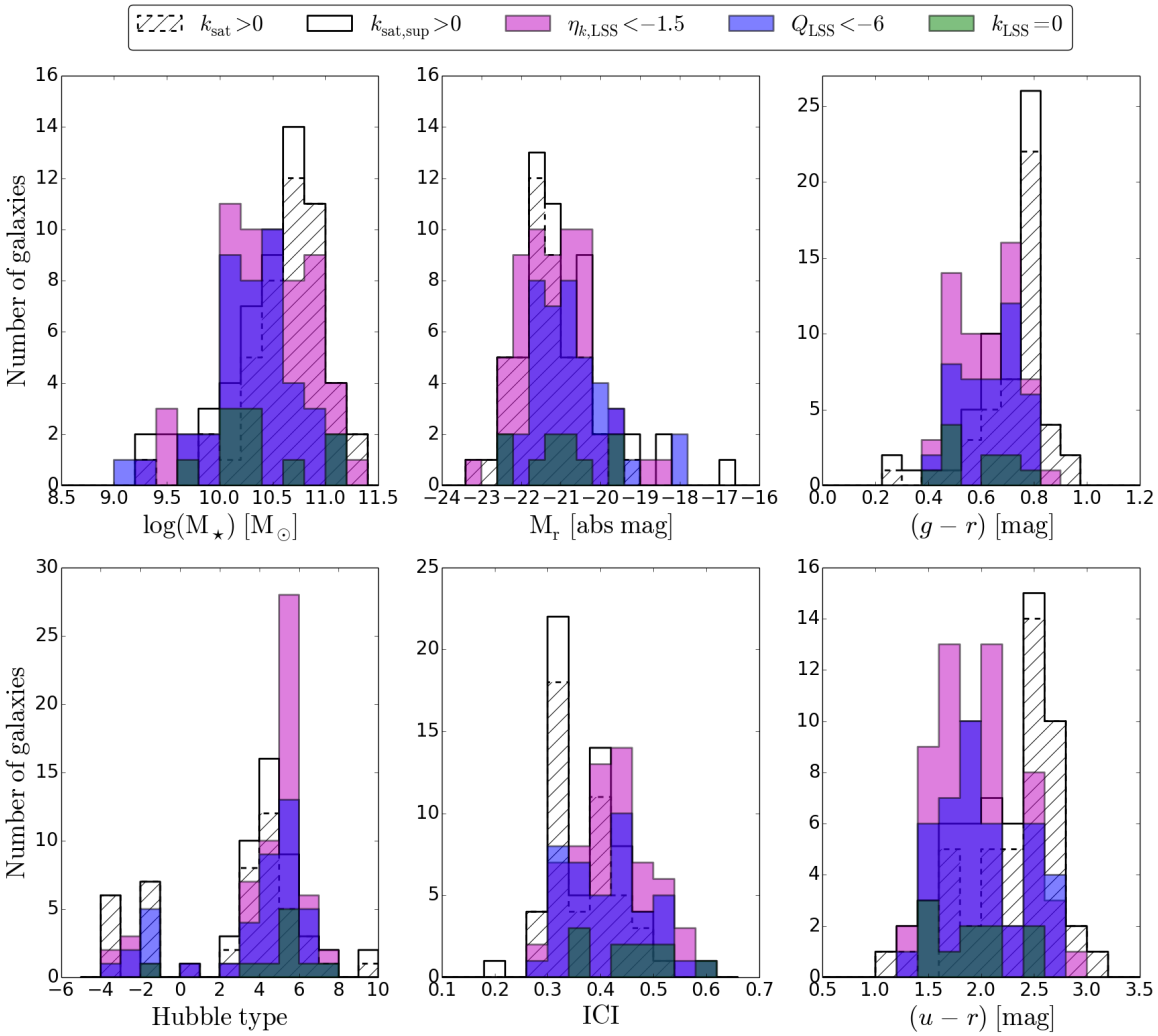

Fig. 9. Distributions of the stellar mass (upper left panel), r-band absolute magnitude (upper central panel), $(g-r)$ rest-frame colour (upper right panel), morphological Hubble type (T) according to Fernández Lorenzo et al. (2012) (lower left panel), inverse concentration index (lower central panel), and $(u-r)$ rest-frame colour (lower right panel) for CIG galaxies. The distributions for the 10 most isolated CIG galaxies are represented by green histograms, and the most isolated CIG galaxies in terms of projected density $\eta_{k,LSS}$ and tidal strength Q_{LSS} are represented by magenta and blue histograms, respectively. On the contrary, distributions for CIG galaxies with satellites are represented by white histograms (hatched histograms for the escape speed selection and plain white histograms in case of upper limit selection of satellites).

the absolute magnitudes of the satellites is comparable for both subsamples, although the most massive early-type CIG galaxies ($M_\star > 10^{10.5}\,M_\odot$) may very marginally attract brighter satellites (see upper panel of Fig. 10). A clearer tendency appears for the distribution of the ICI: massive early-type CIG galaxies will preferentially be surrounded by more early-type companions, with respect to late-type CIG galaxies which will present a higher fraction of late-type satellites (see central panel of Fig. 10). This dichotomy is also seen in the $(g-r)$ colours of the satellites: the satellites are redder, likely have older stellar populations, around massive early-type CIG galaxies while they may present a younger stellar content around massive late-type CIG galaxies, as seen in the lower panel of Fig. 10.

This means that if the local environment has an influence on the evolution of the CIG galaxies, reciprocally, the satellites around the CIG galaxies may also be affected by the nature of the primary galaxy. This suggests that the CIG is composed by an heterogeneous population of galaxies, sampling old systems of galaxies but also spanning more recent, dynamical systems of galaxies.

7. Summary and conclusions

We present a study of the 3-dimensional environment for a sample of 386 galaxies in the **C**atalogue of **I**solated **G**alaxies (CIG; Karachentseva 1973), using the Ninth Data Release of the Sloan Digital Sky Survey (SDSS-DR9).

We identify and quantify the effects of the satellite distribution around a sample of galaxies in the CIG. To recover the physical satellites around the CIG galaxies, we first focus on

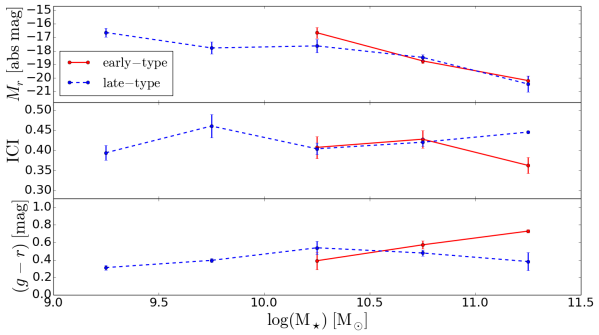

Fig. 10. Mean r-band absolute magnitude (upper panel), ICI (middle panel), and $(g-r)$ rest-frame colour (lower panel) for bound physical satellites as a function of CIG galaxy stellar mass. Mean satellite properties for early-type ($T \leq 0$, red solid line) and late-type ($T > 0$, blue dashed line) CIG galaxies are represented. Error bars are given by the standard deviation.

the satellites which are within the escape speed of each CIG galaxy. We also propose a more conservative method based on the stacked Gaussian distribution of the velocity difference of the neighbours, which gives an upper limit to the influence of the local environment.

In comparison to a previous study (Argudo-Fernández et al. 2013) we can estimate the effect of the physical associations that were not taken into account by the CIG isolation criteria, which could also have a non negligible influence on the evolution of the central CIG galaxy. The tidal strengths affecting the primary galaxy are estimated to quantify the effects of the local and Large Scale Structure (LSS) environments. To characterise the LSS around the CIG galaxies, we define the projected number density parameter at the 5$^{\text{th}}$ nearest neighbour.

Our main conclusions are the following:

1. Out of the 386 CIG galaxies considered in this study, at least 340 (88% of the sample) have no physically linked satellite. Following the more conservative Gaussian distribution method to identify physical satellites around the CIG galaxies leads to upper limits: out of the 386 CIG galaxies, 327 galaxies (85% of the sample) would have no physical companion within a projected distance of 0.3 Mpc.
2. Consequently, about 12% (and up to 15%) of the CIG galaxies have physically bound satellites. CIG galaxies with companions might have a mild tendency (0.3-0.4 dex) to be more massive, which suggests a higher frequency of having suffered a merger in the past. Satellites are in general redder, brighter, and bigger for more massive central CIG galaxies. Also, massive elliptical and lenticular CIG galaxies tend to have satellites with earlier types than similar mass spiral CIG galaxies.
3. Although 15% at most of the CIG galaxies in the sample have physically bound satellite, almost all galaxies (97%) can be directly related to a LSS. The very large scatter in the quantification of the LSS shows that the CIG includes both galaxies dominated by their immediate environment as well as galaxies almost free from any external influence.
4. The continuous distributions of the $\eta_{k,\text{LSS}}$ and Q_{LSS} isolation parameters show that the CIG spans a variety of environments. The connection of the CIG galaxies with the LSS is obvious due to the excess of similar redshift galaxies between 0.3 and 3 Mpc. The CIG galaxies are distributed following the LSS of the local universe, although presenting a large heterogeneity in their degrees of connection with it.
5. To evaluate the role of the physically bound satellites with respect to the large scale environment, we compare the magnitudes of the sum of the tidal strengths produced by the physical companions to the sum of the tidal strengths created by all the galaxies in the LSS. When at least one physical companion is present near a CIG galaxy, its effect largely dominates (usually more than 90%) the tidal strengths generated by the LSS.
6. To delimit the role of the environment on the physical properties of the galaxies we compare, within the CIG, the most isolated galaxies to the galaxies with companions. We find a clear segregation between CIG galaxies with companions and isolated CIG galaxies. Isolated galaxies are in general bluer, with a younger stellar population and rather high star formation with respect to the older, redder galaxies with companions. These $(u-r)$ colours, in combination with the morphological trends and the $(g-r)$ colours, lead to a coherent view where isolated star forming galaxies are separated from older elliptical galaxies with companions.
7. Conjointly, we find that the satellites are redder and with older stellar populations around massive early-type CIG galaxies while they have a younger stellar content around massive late-type CIG galaxies. This means that if the local environment has an influence on the evolution of the CIG galaxies, reciprocally, the satellites around the CIG galaxies may also be affected by the nature of the primary galaxy. This suggests that the CIG is composed of a heterogeneous population of galaxies, sampling old systems of galaxies but also spanning more recent, dynamical systems of galaxies.
8. As mentioned, the CIG samples a variety of environments, from galaxies in interaction with physical satellites to galaxies with no neighbours in the first 3 Mpc around them. Hence, in the construction of catalogues of galaxies in relation to their environments (isolated, pairs, triplets, groups of galaxies), redshift surveys are required in order to distinguish small, faint, physically bound satellites from a background projected galaxy population and reach a more comprehensive 3-dimensional picture of the surroundings.

Acknowledgements. The authors acknowledge the referee for his/her very detailed and useful report, which helped to clarify and improve the quality of this work.

The authors thank J. Jiménez-Vicente for useful discussions.

This work has been supported by Grant AYA2011-30491-C02-01, co-financed by MICINN and FEDER funds, and the Junta de Andaluca (Spain) grants P08-FQM-4205 and TIC-114, as well as under the EU 7th Framework Programme in the area of Digital Libraries and Digital Preservation. (ICT-2009.4.1) Project reference: 270192.

This work was partially supported by a Junta de Andaluca Grant FQM108 and a Spanish MEC Grant AYA-2007-67625-C02-02.

Funding for SDSS-III has been provided by the Alfred P. Sloan Foundation, the Participating Institutions, the National Science Foundation, and the U.S. Department of Energy Office of Science. The SDSS-III web site is http://www.sdss3.org/. SDSS-III is managed by the Astrophysical Research Consortium for the Participating Institutions of the SDSS-III Collaboration including the University of Arizona, the Brazilian Participation Group, Brookhaven National Laboratory, University of Cambridge, University of Florida, the French Participation Group, the German Participation Group, the Instituto de Astrofisica de Canarias, the Michigan State/Notre Dame/JINA Participation Group, Johns Hopkins University, Lawrence Berkeley National Laboratory, Max Planck Institute for Astrophysics, New Mexico State University, New York University, Ohio State University, Pennsylvania State University, University of Portsmouth, Princeton University, the Spanish Participation Group, University of Tokyo, University of Utah, Vanderbilt University, University of Virginia, University of Washington, and Yale University.

This research has made use of data obtained using, or software provided by, the UK's AstroGrid Virtual Observatory Project, which is funded by the

Science and Technology Facilities Council and through the EU's Framework 6 programme. We also acknowledge the use of STILTS and TOPCAT tools Taylor (2005).

This research made use of python (`http://www.python.org`), of Matplotlib (Hunter 2007), a suite of open-source python modules that provides a framework for creating scientific plots.

This research has made use of the NASA/IPAC Extragalactic Database (NED) which is operated by the Jet Propulsion Laboratory, California Institute of Technology, under contract with the National Aeronautics and Space Administration.

We acknowledge the usage of the HyperLeda database (`http://leda.univ-lyon1.fr`) (Paturel et al. 2003).

We thank the SAO/NASA Astrophysics Data System (ADS) that is always so useful.

References

Agustsson, I. & Brainerd, T. G. 2010, ApJ, 709, 1321
Ahn, C. P., Alexandroff, R., Allende Prieto, C., et al. 2012, ApJS, 203, 21
Anderhalden, D., Schneider, A., Macciò, A. V., Diemand, J., & Bertone, G. 2013, J. Cosmology Astropart. Phys., 3, 14
Argudo-Fernández, M., Verley, S., Bergond, G., et al. 2013, A&A, 560, A9
Blanton, M. R. & Roweis, S. 2007, AJ, 133, 734
Bozek, B., Wyse, R. F. G., & Gilmore, G. 2013, ApJ, 772, 109
Choi, J.-H., Weinberg, M. D., & Katz, N. 2007, in Bulletin of the American Astronomical Society, Vol. 39, American Astronomical Society Meeting Abstracts, 126.02
Cooper, M. C., Griffith, R. L., Newman, J. A., et al. 2012, MNRAS, 419, 3018
Dawson, K. S., Schlegel, D. J., Ahn, C. P., et al. 2013, AJ, 145, 10
Diaferio, A. & Geller, M. J. 1997, ApJ, 481, 633
Dressler, A. 1980, ApJ, 236, 351
Dressler, A., Oemler, Jr., A., Couch, W. J., et al. 1997, ApJ, 490, 577
Edman, J. P., Barton, E. J., & Bullock, J. S. 2012, MNRAS, 424, 1454
Einasto, M. & Einasto, J. 1987, MNRAS, 226, 543
Eisenstein, D. J., Weinberg, D. H., Agol, E., et al. 2011, AJ, 142, 72
Fernández Lorenzo, M., Sulentic, J., Verdes-Montenegro, L., & Argudo-Fernández, M. 2013, MNRAS, 434, 325
Fernández Lorenzo, M., Sulentic, J., Verdes-Montenegro, L., et al. 2012, A&A, 540, A47
Ferrero, I., Abadi, M. G., Navarro, J. F., Sales, L. V., & Gurovich, S. 2012, MNRAS, 425, 2817
González, R. E., Kravtsov, A. V., & Gnedin, N. Y. 2013, ApJ, 770, 96
Guo, Q., Cole, S., Eke, V., & Frenk, C. 2011, MNRAS, 417, 370
Guo, Q., Cole, S., Eke, V., & Frenk, C. 2012, MNRAS, 427, 428
Hunter, J. D. 2007, Computing In Science & Engineering, 9, 90
Kaiser, N. 1987, MNRAS, 227, 1
Karachentseva, V. E. 1973, Astrofizicheskie Issledovaniia Izvestiya Spetsial'noj Astrofizicheskoj Observatorii, 8, 3
Karachentseva, V. E., Karachentsev, I. D., & Melnyk, O. V. 2011, Astrophysical Bulletin, 66, 389
Moster, B. P., Naab, T., & White, S. D. M. 2013, MNRAS, 428, 3121
Nair, P. B. & Abraham, R. G. 2010, ApJS, 186, 427
Park, C., Choi, Y., Vogeley, M. S., Gott, I. J. R., & Blanton, M. R. 2007, ApJ, 658, 898
Paturel, G., Petit, C., Prugniel, P., et al. 2003, A&A, 412, 45
Prada, F., Vitvitska, M., Klypin, A., et al. 2003, ApJ, 598, 260
Sabater, J., Best, P. N., & Argudo-Fernández, M. 2013, MNRAS, 430, 638
Sales, L. & Lambas, D. G. 2005, MNRAS, 356, 1045
Schlegel, D. J., Finkbeiner, D. P., & Davis, M. 1998, ApJ, 500, 525
Smee, S., Gunn, J. E., Uomoto, A., et al. 2012, ArXiv e-prints
Strateva, I., Ivezić, Ž., Knapp, G. R., et al. 2001, AJ, 122, 1861
Strauss, M. A., Weinberg, D. H., Lupton, R. H., et al. 2002, AJ, 124, 1810
Strauss, M. A. & Willick, J. A. 1995, Phys. Rep., 261, 271
Sulentic, J. W., Verdes-Montenegro, L., Bergond, G., et al. 2006, A&A, 449, 937
Taylor, M. B. 2005, in Astronomical Society of the Pacific Conference Series, Vol. 347, Astronomical Data Analysis Software and Systems XIV, ed. P. Shopbell, M. Britton, & R. Ebert, 29
Verdes-Montenegro, L., Sulentic, J., Lisenfeld, U., et al. 2005, A&A, 436, 443
Verley, S., Leon, S., Verdes-Montenegro, L., et al. 2007a, A&A, 472, 121
Verley, S., Odewahn, S. C., Verdes-Montenegro, L., et al. 2007b, A&A, 470, 505
York, D. G., Adelman, J., Anderson, J. J. E., et al. 2000, AJ, 120, 1579

Table 1. Quantification of the environment. The columns correspond to: (1) galaxy identification according to the CIG; (2) $Q_{\rm sat}$, tidal strength estimation for satellites using the escape speed method; (3) $Q_{\rm sat,sup}$, tidal strength estimation for satellites using the Gaussian distribution method; (4) $k_{\rm sat}$, number of satellites selected following the escape speed method; (5) $k_{\rm sat,sup}$, number of satellites selected following the Gaussian distribution method; (6) $Q_{\rm LSS}$, tidal strength estimation of the LSS; (7) $\eta_{k,\rm LSS}$, local number density estimation of the LSS; (8) $k_{\rm LSS}$, number of LSS associations; (9) $\frac{Q_{\rm sat}}{Q_{\rm LSS}}$, relation between $Q_{\rm sat}$ and $Q_{\rm LSS}$, from 0 to 1 if the considered satellites amount from 0% to 100% to the total tidal strength; (10) $\frac{Q_{\rm sat,sup}}{Q_{\rm LSS}}$, relation between $Q_{\rm sat,sup}$ and $Q_{\rm LSS}$, from 0 to 1 if the considered satellites amount from 0% to 100% to the total tidal strength.

(1) CIG	(2) $Q_{\rm sat}$	(3) $Q_{\rm sat,sup}$	(4) $k_{\rm sat}$	(5) $k_{\rm sat,sup}$	(6) $Q_{\rm LSS}$	(7) $\eta_{k,\rm LSS}$	(8) $k_{\rm LSS}$	(9) $\frac{Q_{\rm sat}}{Q_{\rm LSS}}$	(10) $\frac{Q_{\rm sat,sup}}{Q_{\rm LSS}}$
11	NULL	NULL	0	0	-6.62	-1.43	5	NULL	NULL
33	NULL	NULL	0	0	-4.80	-0.21	18	NULL	NULL
56	-4.72	-4.72	1	1	-4.22	0.04	37	0.32	0.32
60	NULL	NULL	0	0	-4.76	0.78	31	NULL	NULL
198	-3.31	-3.31	1	1	-3.14	-0.81	11	0.67	0.67
199	NULL	NULL	0	0	-6.10	-0.97	8	NULL	NULL
203	NULL	NULL	0	0	-5.57	-1.94	2	NULL	NULL
204	NULL	NULL	0	0	-3.39	-0.25	18	NULL	NULL
205	NULL	NULL	0	0	-5.21	-1.26	5	NULL	NULL
207	NULL	NULL	0	0	-4.23	-0.36	27	NULL	NULL
210	NULL	NULL	0	0	-3.86	-1.32	7	NULL	NULL
211	-3.47	-3.47	2	2	-3.47	-1.23	6	0.99	0.99
212	NULL	NULL	0	0	-6.12	-0.58	14	NULL	NULL
213	NULL	NULL	0	0	-5.06	-0.41	3	NULL	NULL
214	NULL	NULL	0	0	-5.74	-1.53	4	NULL	NULL
216	NULL	NULL	0	0	-6.57	-1.95	2	NULL	NULL
217	NULL	NULL	0	0	-5.71	-1.62	3	NULL	NULL
219	NULL	NULL	0	0	-4.26	-1.09	7	NULL	NULL
220	NULL	NULL	0	0	-4.75	-1.32	7	NULL	NULL
221	NULL	NULL	0	0	-4.27	-1.15	7	NULL	NULL
222	NULL	NULL	0	0	-5.05	-1.40	4	NULL	NULL
223	NULL	NULL	0	0	-4.78	-1.70	3	NULL	NULL
225	NULL	NULL	0	0	-3.71	-1.40	5	NULL	NULL
226	NULL	NULL	0	0	-4.17	-0.86	9	NULL	NULL
227	NULL	NULL	0	0	-3.70	-1.10	7	NULL	NULL
228	-4.65	-4.65	1	1	-4.43	-0.22	19	0.60	0.60
229	NULL	NULL	0	0	NULL	NULL	0	NULL	NULL
231	NULL	NULL	0	0	-5.00	-0.77	7	NULL	NULL
232	-2.50	-2.50	2	2	-2.50	-0.60	17	1.00	1.00
233	NULL	NULL	0	0	-4.55	-0.89	10	NULL	NULL
234	NULL	NULL	0	0	-5.34	-2.01	2	NULL	NULL
236	NULL	NULL	0	0	-6.53	-2.03	2	NULL	NULL
237	-3.17	-3.15	2	3	-3.10	0.84	20	0.84	0.88
238	NULL	NULL	0	0	-4.04	-1.27	11	NULL	NULL
241	NULL	NULL	0	0	-4.48	-0.96	7	NULL	NULL
242	NULL	NULL	0	0	-4.50	-0.81	36	NULL	NULL
243	NULL	NULL	0	0	-4.33	-0.19	56	NULL	NULL
244	NULL	NULL	0	0	-4.38	-0.14	29	NULL	NULL
245	NULL	NULL	0	0	NULL	NULL	0	NULL	NULL
247	NULL	NULL	0	0	-5.79	-1.05	14	NULL	NULL
248	NULL	NULL	0	0	-6.15	-1.34	4	NULL	NULL
249	NULL	NULL	0	0	-6.16	-1.44	2	NULL	NULL
250	-3.62	-3.51	1	2	-3.51	-0.25	8	0.76	0.99
252	NULL	NULL	0	0	-2.90	-0.49	14	NULL	NULL
254	NULL	NULL	0	0	-4.37	-1.12	3	NULL	NULL
257	NULL	NULL	0	0	-4.73	-1.40	6	NULL	NULL
258	NULL	NULL	0	0	-4.95	-0.86	11	NULL	NULL
260	NULL	NULL	0	0	-4.32	-0.75	16	NULL	NULL
261	NULL	NULL	0	0	-4.47	-1.47	4	NULL	NULL
262	NULL	NULL	0	0	-5.63	-0.86	19	NULL	NULL
263	NULL	NULL	0	0	-4.23	-0.55	19	NULL	NULL
264	NULL	NULL	0	0	-5.06	-0.77	12	NULL	NULL
268	NULL	NULL	0	0	-4.07	-0.50	25	NULL	NULL
269	NULL	NULL	0	0	-3.97	-1.08	8	NULL	NULL

Table 1. Continued.

(1)	(2)	(3)	(4)	(5)	(6)	(7)	(8)	(9)	(10)
CIG	$Q_{\rm sat}$	$Q_{\rm sat,sup}$	$k_{\rm sat}$	$k_{\rm sat,sup}$	$Q_{\rm LSS}$	$\eta_{k,\rm LSS}$	$k_{\rm LSS}$	$\frac{Q_{\rm sat}}{Q_{\rm LSS}}$	$\frac{Q_{\rm sat,sup}}{Q_{\rm LSS}}$
270	NULL	-3.94	0	1	-2.94	-1.16	8	NULL	0.10
271	NULL	NULL	0	0	-4.41	-0.47	13	NULL	NULL
272	NULL	NULL	0	0	-6.53	-1.93	2	NULL	NULL
273	NULL	NULL	0	0	-3.52	-0.44	18	NULL	NULL
274	-4.58	-4.58	1	1	-4.52	-1.39	5	0.89	0.89
276	NULL	NULL	0	0	-5.46	-1.12	7	NULL	NULL
278	-3.91	-3.91	1	1	-3.86	-1.21	5	0.89	0.89
279	NULL	NULL	0	0	-5.26	-0.50	9	NULL	NULL
280	NULL	NULL	0	0	-4.33	-1.03	17	NULL	NULL
281	NULL	NULL	0	0	-6.77	-1.35	4	NULL	NULL
282	NULL	NULL	0	0	-3.91	-0.49	15	NULL	NULL
283	NULL	NULL	0	0	-4.30	-0.40	9	NULL	NULL
284	NULL	NULL	0	0	NULL	NULL	0	NULL	NULL
286	NULL	NULL	0	0	-4.64	-1.75	3	NULL	NULL
287	NULL	NULL	0	0	-4.86	-1.01	8	NULL	NULL
288	NULL	NULL	0	0	-6.31	NULL	1	NULL	NULL
289	NULL	NULL	0	0	-4.82	-1.23	11	NULL	NULL
290	NULL	NULL	0	0	-4.86	-0.79	16	NULL	NULL
292	NULL	NULL	0	0	-5.33	-0.16	17	NULL	NULL
293	NULL	-4.38	0	1	-4.16	-1.11	14	NULL	0.60
294	NULL	NULL	0	0	-4.00	-0.66	9	NULL	NULL
296	NULL	-2.80	0	1	-2.79	-1.22	8	NULL	0.98
298	NULL	NULL	0	0	-4.14	-0.42	25	NULL	NULL
299	NULL	NULL	0	0	-4.33	0.38	35	NULL	NULL
302	NULL	NULL	0	0	-4.04	0.06	54	NULL	NULL
303	-3.51	-3.51	2	2	-3.47	0.06	27	0.91	0.91
304	NULL	NULL	0	0	-3.22	-0.97	11	NULL	NULL
305	NULL	NULL	0	0	-6.02	-1.21	7	NULL	NULL
306	NULL	NULL	0	0	-5.52	-1.97	2	NULL	NULL
307	NULL	NULL	0	0	-5.78	NULL	1	NULL	NULL
308	NULL	NULL	0	0	-3.40	0.80	49	NULL	NULL
310	NULL	NULL	0	0	-4.45	-0.90	6	NULL	NULL
311	NULL	NULL	0	0	-5.55	-1.74	2	NULL	NULL
312	NULL	NULL	0	0	-3.89	-0.56	15	NULL	NULL
313	NULL	NULL	0	0	-5.69	-1.61	3	NULL	NULL
314	NULL	NULL	0	0	-5.67	-0.82	14	NULL	NULL
316	NULL	NULL	0	0	-4.27	-0.28	22	NULL	NULL
317	NULL	NULL	0	0	-5.47	-1.20	14	NULL	NULL
318	NULL	NULL	0	0	NULL	NULL	0	NULL	NULL
319	-3.73	-3.73	2	2	-3.60	-0.02	11	0.75	0.75
321	NULL	NULL	0	0	-4.43	NULL	1	NULL	NULL
322	NULL	NULL	0	0	-6.38	-0.72	17	NULL	NULL
323	-3.60	-3.60	1	1	-3.54	-0.75	12	0.86	0.86
325	NULL	NULL	0	0	-6.04	-1.35	7	NULL	NULL
327	NULL	NULL	0	0	-4.98	-0.56	27	NULL	NULL
328	NULL	NULL	0	0	-5.47	0.05	12	NULL	NULL
329	NULL	NULL	0	0	-5.68	-1.41	5	NULL	NULL
330	NULL	NULL	0	0	-3.61	-0.48	15	NULL	NULL
331	NULL	NULL	0	0	NULL	NULL	0	NULL	NULL
332	NULL	NULL	0	0	-4.74	-0.31	16	NULL	NULL
333	NULL	NULL	0	0	-3.81	-1.70	3	NULL	NULL
334	NULL	NULL	0	0	-4.77	-0.63	28	NULL	NULL
335	NULL	NULL	0	0	-4.87	-0.55	9	NULL	NULL
336	NULL	NULL	0	0	-3.14	0.22	28	NULL	NULL
337	NULL	NULL	0	0	-3.94	-0.84	9	NULL	NULL
338	-6.03	-6.03	1	1	-5.67	-0.17	14	0.44	0.44
339	NULL	-3.07	0	1	-2.98	-0.37	10	NULL	0.80
340	NULL	NULL	0	0	-3.93	-0.79	17	NULL	NULL
341	NULL	NULL	0	0	-3.89	-1.12	3	NULL	NULL
342	NULL	NULL	0	0	-4.57	-0.87	18	NULL	NULL

Table 1. Continued.

(1)	(2)	(3)	(4)	(5)	(6)	(7)	(8)	(9)	(10)
CIG	$Q_{\rm sat}$	$Q_{\rm sat,sup}$	$k_{\rm sat}$	$k_{\rm sat,sup}$	$Q_{\rm LSS}$	$\eta_{k,\rm LSS}$	$k_{\rm LSS}$	$\frac{Q_{\rm sat}}{Q_{\rm LSS}}$	$\frac{Q_{\rm sat,sup}}{Q_{\rm LSS}}$
343	NULL	NULL	0	0	-3.42	-0.12	12	NULL	NULL
344	NULL	NULL	0	0	-4.82	-1.01	9	NULL	NULL
348	-2.85	-2.85	1	1	-2.85	-1.33	3	1.00	1.00
349	NULL	NULL	0	0	-5.15	-1.14	6	NULL	NULL
350	NULL	NULL	0	0	-4.36	-1.45	5	NULL	NULL
351	NULL	NULL	0	0	-4.99	-1.17	5	NULL	NULL
352	NULL	NULL	0	0	-5.34	-0.42	49	NULL	NULL
353	NULL	NULL	0	0	-4.51	-0.78	11	NULL	NULL
355	-4.00	-4.00	1	1	-3.91	-0.28	11	0.83	0.83
358	NULL	NULL	0	0	-5.98	-0.69	8	NULL	NULL
359	NULL	NULL	0	0	-5.49	-1.31	4	NULL	NULL
360	NULL	NULL	0	0	-4.57	-1.06	8	NULL	NULL
361	NULL	NULL	0	0	-4.31	-0.28	16	NULL	NULL
364	NULL	NULL	0	0	-5.38	-1.27	7	NULL	NULL
365	NULL	NULL	0	0	-4.02	-0.68	9	NULL	NULL
366	NULL	NULL	0	0	-4.36	-0.76	23	NULL	NULL
367	-2.69	-2.69	1	1	-2.67	-0.40	7	0.97	0.97
368	NULL	NULL	0	0	-4.25	-1.75	2	NULL	NULL
370	NULL	NULL	0	0	-5.24	-1.74	3	NULL	NULL
372	NULL	NULL	0	0	-4.96	-1.32	5	NULL	NULL
373	NULL	NULL	0	0	-4.12	-0.84	6	NULL	NULL
374	NULL	NULL	0	0	-5.11	-1.47	4	NULL	NULL
375	NULL	NULL	0	0	-4.17	-1.35	7	NULL	NULL
378	NULL	NULL	0	0	-6.44	-1.63	2	NULL	NULL
379	NULL	NULL	0	0	-4.36	-0.86	11	NULL	NULL
380	NULL	NULL	0	0	-5.61	-0.54	4	NULL	NULL
381	NULL	NULL	0	0	-5.51	-0.81	14	NULL	NULL
384	NULL	NULL	0	0	-4.12	-1.04	3	NULL	NULL
385	-4.88	-4.88	1	1	-4.27	-0.13	16	0.25	0.25
386	NULL	NULL	0	0	-5.64	-1.42	5	NULL	NULL
387	NULL	NULL	0	0	-5.99	-1.32	4	NULL	NULL
391	NULL	NULL	0	0	-4.16	-1.55	4	NULL	NULL
392	NULL	NULL	0	0	-5.09	-1.27	7	NULL	NULL
394	NULL	NULL	0	0	-4.05	-0.99	13	NULL	NULL
395	NULL	NULL	0	0	-4.60	-1.61	3	NULL	NULL
397	NULL	NULL	0	0	-5.22	0.45	18	NULL	NULL
398	NULL	NULL	0	0	-4.07	-1.06	7	NULL	NULL
399	NULL	NULL	0	0	-5.54	-1.33	8	NULL	NULL
400	-3.53	-3.53	2	2	-3.53	-0.96	9	0.99	0.99
401	-1.76	-1.76	1	1	-1.76	-0.76	19	1.00	1.00
403	NULL	NULL	0	0	-3.78	-0.57	11	NULL	NULL
405	NULL	NULL	0	0	-5.00	-0.56	15	NULL	NULL
406	NULL	NULL	0	0	-5.63	-1.18	10	NULL	NULL
408	NULL	NULL	0	0	-3.89	-1.08	2	NULL	NULL
409	NULL	NULL	0	0	-3.67	0.50	38	NULL	NULL
410	NULL	NULL	0	0	-4.23	-0.53	25	NULL	NULL
412	NULL	NULL	0	0	-3.89	-0.71	8	NULL	NULL
413	NULL	NULL	0	0	-4.66	0.39	23	NULL	NULL
414	NULL	NULL	0	0	-5.07	-1.29	5	NULL	NULL
415	NULL	NULL	0	0	-4.70	-1.20	5	NULL	NULL
416	NULL	-4.42	0	2	-4.41	-1.50	4	NULL	0.98
417	NULL	NULL	0	0	-5.28	-1.29	8	NULL	NULL
418	NULL	NULL	0	0	-5.77	-0.85	11	NULL	NULL
419	NULL	NULL	0	0	-5.19	-1.64	3	NULL	NULL
420	NULL	NULL	0	0	-6.22	-0.96	10	NULL	NULL
423	-1.80	-1.80	2	2	-1.80	-0.46	23	1.00	1.00
424	NULL	NULL	0	0	-4.01	-0.62	19	NULL	NULL
425	NULL	NULL	0	0	-4.08	-0.46	17	NULL	NULL
426	NULL	NULL	0	0	-4.95	-0.74	27	NULL	NULL
427	NULL	NULL	0	0	-6.09	-1.71	3	NULL	NULL

Table 1. Continued.

(1)	(2)	(3)	(4)	(5)	(6)	(7)	(8)	(9)	(10)
CIG	$Q_{\rm sat}$	$Q_{\rm sat,sup}$	$k_{\rm sat}$	$k_{\rm sat,sup}$	$Q_{\rm LSS}$	$\eta_{k,\rm LSS}$	$k_{\rm LSS}$	$\frac{Q_{\rm sat}}{Q_{\rm LSS}}$	$\frac{Q_{\rm sat,sup}}{Q_{\rm LSS}}$
430	NULL	NULL	0	0	-4.32	-0.68	8	NULL	NULL
431	NULL	NULL	0	0	-5.42	-1.05	2	NULL	NULL
432	NULL	NULL	0	0	-4.29	-1.39	5	NULL	NULL
437	-3.70	-3.70	1	1	-3.69	-0.88	16	0.98	0.98
438	NULL	NULL	0	0	-3.35	-0.02	14	NULL	NULL
439	NULL	NULL	0	0	-3.39	-0.34	31	NULL	NULL
440	NULL	NULL	0	0	-2.68	0.26	11	NULL	NULL
441	NULL	NULL	0	0	-4.75	-0.53	13	NULL	NULL
443	NULL	NULL	0	0	-6.10	-1.11	10	NULL	NULL
445	NULL	NULL	0	0	-3.72	-0.45	10	NULL	NULL
446	NULL	NULL	0	0	-4.49	-0.42	16	NULL	NULL
450	NULL	NULL	0	0	-4.35	-0.66	12	NULL	NULL
451	NULL	NULL	0	0	-7.09	NULL	1	NULL	NULL
453	NULL	NULL	0	0	-4.21	-0.23	36	NULL	NULL
456	NULL	NULL	0	0	-5.72	-1.70	3	NULL	NULL
457	NULL	NULL	0	0	-7.35	NULL	1	NULL	NULL
458	NULL	NULL	0	0	-5.06	-1.52	4	NULL	NULL
459	NULL	NULL	0	0	-5.67	-1.67	3	NULL	NULL
460	NULL	NULL	0	0	-4.87	-1.00	10	NULL	NULL
462	NULL	NULL	0	0	-5.29	-0.68	17	NULL	NULL
463	NULL	NULL	0	0	-4.77	-0.66	11	NULL	NULL
466	NULL	NULL	0	0	-4.53	-1.41	7	NULL	NULL
467	NULL	NULL	0	0	-4.79	-1.01	6	NULL	NULL
468	NULL	NULL	0	0	-5.21	-0.69	7	NULL	NULL
473	NULL	NULL	0	0	-5.16	-1.27	6	NULL	NULL
474	NULL	-2.74	0	1	-2.72	-0.43	10	NULL	0.97
475	NULL	NULL	0	0	-4.59	-1.41	3	NULL	NULL
476	NULL	NULL	0	0	-5.68	-1.08	17	NULL	NULL
478	NULL	NULL	0	0	-3.90	-0.89	10	NULL	NULL
479	NULL	NULL	0	0	-5.21	-1.46	3	NULL	NULL
480	NULL	NULL	0	0	-4.85	-0.79	12	NULL	NULL
482	NULL	NULL	0	0	-4.19	-1.43	3	NULL	NULL
485	NULL	NULL	0	0	-5.56	-0.84	8	NULL	NULL
487	NULL	NULL	0	0	-4.89	-1.09	8	NULL	NULL
489	NULL	NULL	0	0	-4.80	-0.64	12	NULL	NULL
490	NULL	NULL	0	0	-5.70	-1.36	8	NULL	NULL
491	NULL	NULL	0	0	-7.10	-1.29	3	NULL	NULL
492	NULL	NULL	0	0	-5.57	-1.15	9	NULL	NULL
493	NULL	NULL	0	0	-4.16	NULL	1	NULL	NULL
494	NULL	NULL	0	0	-3.98	-0.51	15	NULL	NULL
495	NULL	-4.96	0	1	-4.94	-0.85	11	NULL	0.95
497	NULL	NULL	0	0	-5.79	-1.57	3	NULL	NULL
499	NULL	NULL	0	0	-5.22	-1.30	4	NULL	NULL
500	NULL	NULL	0	0	-4.73	-1.12	12	NULL	NULL
501	NULL	NULL	0	0	-6.96	NULL	1	NULL	NULL
504	NULL	NULL	0	0	-4.89	-0.50	9	NULL	NULL
507	NULL	NULL	0	0	-4.24	-0.79	14	NULL	NULL
508	NULL	NULL	0	0	-4.69	-0.94	11	NULL	NULL
510	NULL	NULL	0	0	-4.75	-0.84	21	NULL	NULL
513	NULL	NULL	0	0	-4.43	-1.50	4	NULL	NULL
515	NULL	NULL	0	0	-4.45	-0.75	43	NULL	NULL
516	NULL	NULL	0	0	-4.20	-0.49	17	NULL	NULL
517	-3.83	-3.83	1	1	-3.76	-0.80	4	0.86	0.86
519	NULL	NULL	0	0	-5.58	NULL	1	NULL	NULL
520	-4.42	-4.42	1	1	-4.42	-1.73	2	1.00	1.00
521	NULL	NULL	0	0	-5.24	-0.29	71	NULL	NULL
522	NULL	NULL	0	0	-6.79	-1.47	4	NULL	NULL
525	NULL	NULL	0	0	-4.70	-0.61	18	NULL	NULL
526	NULL	NULL	0	0	-4.87	-1.27	5	NULL	NULL
528	-4.54	-4.54	1	1	-4.27	-0.89	10	0.53	0.53

Table 1. Continued.

(1)	(2)	(3)	(4)	(5)	(6)	(7)	(8)	(9)	(10)
CIG	$Q_{\rm sat}$	$Q_{\rm sat,sup}$	$k_{\rm sat}$	$k_{\rm sat,sup}$	$Q_{\rm LSS}$	$\eta_{k,\rm LSS}$	$k_{\rm LSS}$	$\frac{Q_{\rm sat}}{Q_{\rm LSS}}$	$\frac{Q_{\rm sat,sup}}{Q_{\rm LSS}}$
529	NULL	NULL	0	0	-5.94	-1.29	6	NULL	NULL
532	NULL	NULL	0	0	-5.21	-1.28	6	NULL	NULL
537	NULL	NULL	0	0	-6.72	-1.46	3	NULL	NULL
539	-3.09	-3.09	1	1	-3.09	-1.21	4	1.00	1.00
541	NULL	NULL	0	0	NULL	NULL	0	NULL	NULL
542	NULL	NULL	0	0	NULL	NULL	0	NULL	NULL
544	NULL	NULL	0	0	-5.77	-1.42	6	NULL	NULL
545	NULL	NULL	0	0	-5.05	-0.93	8	NULL	NULL
546	NULL	NULL	0	0	NULL	NULL	0	NULL	NULL
548	NULL	NULL	0	0	-5.24	-0.34	12	NULL	NULL
550	NULL	NULL	0	0	-4.72	-0.87	9	NULL	NULL
553	NULL	NULL	0	0	-4.38	-0.42	31	NULL	NULL
554	-3.13	-3.13	1	1	-3.11	-0.96	12	0.97	0.97
557	-2.65	-2.65	2	2	-2.65	0.14	7	0.99	0.99
558	NULL	NULL	0	0	-5.14	-1.41	5	NULL	NULL
560	NULL	NULL	0	0	-5.55	-1.19	7	NULL	NULL
561	NULL	NULL	0	0	-5.22	0.17	26	NULL	NULL
563	NULL	NULL	0	0	-4.12	-1.08	11	NULL	NULL
565	NULL	NULL	0	0	-3.94	-0.35	22	NULL	NULL
566	NULL	NULL	0	0	-4.80	-0.61	17	NULL	NULL
567	NULL	NULL	0	0	-4.53	-1.15	5	NULL	NULL
568	NULL	NULL	0	0	-3.23	0.07	14	NULL	NULL
570	NULL	NULL	0	0	-5.94	-1.33	8	NULL	NULL
571	NULL	NULL	0	0	-5.29	-0.58	13	NULL	NULL
572	NULL	NULL	0	0	-3.35	-0.29	18	NULL	NULL
575	NULL	NULL	0	0	-4.61	0.22	16	NULL	NULL
576	NULL	NULL	0	0	-4.17	-0.31	27	NULL	NULL
578	-4.47	-4.47	1	1	-4.45	-1.06	5	0.96	0.96
579	NULL	NULL	0	0	-4.15	-0.38	41	NULL	NULL
580	NULL	NULL	0	0	-4.39	-0.62	32	NULL	NULL
581	NULL	NULL	0	0	-3.39	-0.19	24	NULL	NULL
582	NULL	NULL	0	0	-4.90	-1.52	4	NULL	NULL
583	NULL	NULL	0	0	-4.02	-0.57	7	NULL	NULL
585	NULL	NULL	0	0	-4.61	-0.95	15	NULL	NULL
586	NULL	NULL	0	0	-4.73	-0.76	24	NULL	NULL
587	NULL	NULL	0	0	-4.58	-0.98	5	NULL	NULL
589	-2.98	-2.98	1	1	-2.97	-1.04	5	0.98	0.98
591	NULL	NULL	0	0	-4.73	-0.41	25	NULL	NULL
592	NULL	-5.13	0	1	-4.51	0.22	41	NULL	0.24
594	NULL	NULL	0	0	-4.85	-1.54	4	NULL	NULL
595	-0.40	-0.40	1	1	-0.40	-0.04	22	1.00	1.00
596	-3.71	-3.71	1	1	-3.14	0.28	26	0.27	0.27
598	NULL	NULL	0	0	-5.34	-1.43	5	NULL	NULL
599	NULL	NULL	0	0	-4.78	-1.23	5	NULL	NULL
600	NULL	NULL	0	0	-3.35	0.07	18	NULL	NULL
601	NULL	NULL	0	0	-4.38	-1.18	11	NULL	NULL
602	NULL	NULL	0	0	-3.57	-1.08	8	NULL	NULL
603	NULL	NULL	0	0	-4.37	-0.89	16	NULL	NULL
605	-3.58	-3.58	1	1	-3.58	-1.02	9	1.00	1.00
606	-1.80	-1.80	1	1	-1.80	-1.62	3	1.00	1.00
607	NULL	NULL	0	0	-3.88	-0.67	18	NULL	NULL
608	NULL	NULL	0	0	-5.46	NULL	1	NULL	NULL
609	NULL	-4.52	0	2	-4.21	0.69	55	NULL	0.49
611	NULL	NULL	0	0	-3.77	0.20	35	NULL	NULL
612	-3.06	-3.06	1	1	-3.04	-0.74	8	0.94	0.94
613	NULL	NULL	0	0	-4.13	-1.13	3	NULL	NULL
614	NULL	NULL	0	0	-2.89	-0.35	11	NULL	NULL
616	NULL	NULL	0	0	-4.97	-1.40	4	NULL	NULL
617	NULL	NULL	0	0	-5.51	-1.31	5	NULL	NULL
618	-2.47	-2.47	1	1	-2.47	-1.59	3	1.00	1.00

Table 1. Continued.

(1)	(2)	(3)	(4)	(5)	(6)	(7)	(8)	(9)	(10)
CIG	$Q_{\rm sat}$	$Q_{\rm sat,sup}$	$k_{\rm sat}$	$k_{\rm sat,sup}$	$Q_{\rm LSS}$	$\eta_{k,\rm LSS}$	$k_{\rm LSS}$	$\frac{Q_{\rm sat}}{Q_{\rm LSS}}$	$\frac{Q_{\rm sat,sup}}{Q_{\rm LSS}}$
619	NULL	NULL	0	0	-3.38	-1.08	5	NULL	NULL
620	NULL	NULL	0	0	-5.35	-1.40	5	NULL	NULL
622	NULL	NULL	0	0	-5.82	-0.74	19	NULL	NULL
623	NULL	NULL	0	0	-5.14	-0.97	14	NULL	NULL
625	NULL	-3.12	0	1	-3.08	-0.15	26	NULL	0.91
626	NULL	NULL	0	0	-4.10	0.16	71	NULL	NULL
628	NULL	NULL	0	0	-3.79	-1.38	5	NULL	NULL
630	NULL	-4.90	0	1	-4.89	-0.74	11	NULL	0.96
631	NULL	NULL	0	0	-5.42	0.56	54	NULL	NULL
633	NULL	NULL	0	0	-4.62	0.12	65	NULL	NULL
634	-3.48	-3.48	1	1	-3.48	0.51	87	0.99	0.99
635	NULL	NULL	0	0	-3.74	-0.40	16	NULL	NULL
636	NULL	NULL	0	0	-6.63	NULL	1	NULL	NULL
637	-3.54	-3.54	1	1	-3.54	-0.26	78	1.00	1.00
639	NULL	NULL	0	0	-4.58	-0.77	13	NULL	NULL
640	NULL	NULL	0	0	-5.70	-1.61	3	NULL	NULL
641	NULL	NULL	0	0	-6.88	NULL	1	NULL	NULL
643	NULL	NULL	0	0	-3.89	-0.40	20	NULL	NULL
644	-4.12	-4.12	1	1	-4.07	-1.34	7	0.89	0.89
645	NULL	NULL	0	0	-4.57	-1.18	11	NULL	NULL
646	NULL	NULL	0	0	-5.08	-1.05	3	NULL	NULL
647	NULL	NULL	0	0	-3.82	-1.02	8	NULL	NULL
648	NULL	NULL	0	0	-4.17	-0.91	27	NULL	NULL
650	NULL	NULL	0	0	-3.74	-0.34	25	NULL	NULL
653	-4.68	-4.68	1	1	-4.17	-0.25	15	0.31	0.31
655	NULL	NULL	0	0	-4.67	-0.82	13	NULL	NULL
658	NULL	NULL	0	0	-3.89	-0.48	22	NULL	NULL
659	NULL	NULL	0	0	-4.31	-1.43	5	NULL	NULL
665	NULL	NULL	0	0	-4.81	-0.76	9	NULL	NULL
667	NULL	NULL	0	0	-6.08	-1.43	4	NULL	NULL
668	NULL	NULL	0	0	-4.10	-0.85	21	NULL	NULL
672	NULL	NULL	0	0	-4.50	-1.58	3	NULL	NULL
674	NULL	NULL	0	0	NULL	NULL	0	NULL	NULL
675	NULL	NULL	0	0	-4.71	-0.77	20	NULL	NULL
676	NULL	NULL	0	0	-5.09	-1.01	4	NULL	NULL
678	NULL	NULL	0	0	-5.44	-1.41	5	NULL	NULL
679	NULL	NULL	0	0	-6.35	-1.72	3	NULL	NULL
680	NULL	NULL	0	0	-4.24	-0.76	26	NULL	NULL
681	NULL	NULL	0	0	-5.56	-1.41	5	NULL	NULL
683	NULL	NULL	0	0	-4.35	-0.79	18	NULL	NULL
685	NULL	NULL	0	0	-4.54	-1.64	3	NULL	NULL
689	NULL	NULL	0	0	-5.07	-0.87	10	NULL	NULL
690	NULL	NULL	0	0	-6.82	-1.55	4	NULL	NULL
693	NULL	NULL	0	0	-5.58	-1.40	6	NULL	NULL
694	-2.89	-2.89	1	1	-2.89	-1.48	3	1.00	1.00
695	NULL	NULL	0	0	-4.27	-0.61	17	NULL	NULL
696	NULL	-2.37	0	1	-2.37	-0.56	7	NULL	1.00
698	NULL	NULL	0	0	-6.46	-1.12	4	NULL	NULL
701	-1.11	-1.11	1	1	-1.11	0.82	2	1.00	1.00
702	NULL	NULL	0	0	NULL	NULL	0	NULL	NULL
703	-6.07	-6.07	1	1	-6.01	-1.38	4	0.89	0.89
704	NULL	NULL	0	0	-4.28	-0.21	22	NULL	NULL
705	NULL	NULL	0	0	-5.64	-0.69	9	NULL	NULL
714	NULL	NULL	0	0	-4.87	-0.49	36	NULL	NULL
716	NULL	NULL	0	0	-3.99	-1.44	5	NULL	NULL
717	NULL	NULL	0	0	-4.55	-1.18	8	NULL	NULL
719	NULL	NULL	0	0	-3.19	-0.50	26	NULL	NULL
721	-3.66	-3.66	2	2	-3.32	0.36	18	0.45	0.45
722	-3.69	-3.69	1	1	-3.68	-0.32	8	0.98	0.98
723	NULL	NULL	0	0	-3.82	-0.42	14	NULL	NULL

Table 1. Continued.

(1) CIG	(2) $Q_{\rm sat}$	(3) $Q_{\rm sat,sup}$	(4) $k_{\rm sat}$	(5) $k_{\rm sat,sup}$	(6) $Q_{\rm LSS}$	(7) $\eta_{k,\rm LSS}$	(8) $k_{\rm LSS}$	(9) $\frac{Q_{\rm sat}}{Q_{\rm LSS}}$	(10) $\frac{Q_{\rm sat,sup}}{Q_{\rm LSS}}$
724	NULL	NULL	0	0	-3.15	-0.85	17	NULL	NULL
725	NULL	NULL	0	0	-4.98	-1.41	6	NULL	NULL
726	NULL	NULL	0	0	-3.56	-0.31	43	NULL	NULL
731	NULL	NULL	0	0	-4.53	-1.16	15	NULL	NULL
733	NULL	NULL	0	0	-4.93	-0.15	14	NULL	NULL
735	NULL	NULL	0	0	-4.39	0.05	40	NULL	NULL
739	NULL	-3.90	0	1	-3.82	-0.98	4	NULL	0.83
741	NULL	NULL	0	0	-3.84	-1.54	4	NULL	NULL
743	NULL	NULL	0	0	-7.53	NULL	1	NULL	NULL
747	NULL	NULL	0	0	-3.12	-1.19	6	NULL	NULL
749	NULL	NULL	0	0	-5.13	-1.06	6	NULL	NULL
751	NULL	NULL	0	0	-5.38	-0.63	13	NULL	NULL
752	NULL	NULL	0	0	-5.58	-1.42	4	NULL	NULL
757	NULL	NULL	0	0	-4.71	-0.60	8	NULL	NULL
761	NULL	NULL	0	0	-5.98	NULL	1	NULL	NULL
762	NULL	NULL	0	0	-5.01	-0.36	6	NULL	NULL
767	NULL	NULL	0	0	-4.89	-2.04	2	NULL	NULL
771	0.11	0.11	3	3	0.11	0.85	30	1.00	1.00
780	NULL	NULL	0	0	-4.88	0.06	2	NULL	NULL
795	NULL	NULL	0	0	-4.20	-0.93	23	NULL	NULL
807	NULL	NULL	0	0	-5.35	-1.29	6	NULL	NULL
893	NULL	NULL	0	0	-4.50	-0.37	43	NULL	NULL
924	-3.24	-3.24	1	1	-3.23	-0.54	11	0.99	0.99
931	NULL	NULL	0	0	-5.15	-0.63	19	NULL	NULL
932	NULL	NULL	0	0	-4.71	-0.65	13	NULL	NULL
937	NULL	NULL	0	0	-4.18	-0.07	21	NULL	NULL
943	NULL	NULL	0	0	-7.86	-1.59	2	NULL	NULL
980	NULL	NULL	0	0	-5.42	-1.48	2	NULL	NULL
1008	NULL	NULL	0	0	-4.87	-1.71	3	NULL	NULL
1014	NULL	NULL	0	0	-5.71	-1.72	3	NULL	NULL
1029	NULL	NULL	0	0	-4.90	NULL	1	NULL	NULL
1030	NULL	NULL	0	0	-4.52	-0.82	16	NULL	NULL